Drug-target Mendelian randomization analysis supports lowering plasma ANGPTL3, ANGPTL4, and APOC3 levels as strategies for reducing cardiovascular disease risk

Fredrik Landfors[1, 2, *], Stefan K. Nilsson[2, 3], Sander Kersten[4, 5]

[1] Department of Public Health and Clinical Medicine, Section of Medicine, Umeå University, Umeå, Sweden.

[2] Lipigon Pharmaceuticals AB, Umeå, Sweden.

[3] Department of Medical Biosciences, Umea□ University, Umea□, Sweden

[4] Nutrition, Metabolism, and Genomics group, Division of Human Nutrition and Health, Wageningen University, 6708WE, Wageningen, the Netherlands.

[5] Division of Nutritional Sciences, Cornell University, Ithaca, NY 14853, USA.

[*] To whom correspondence should be addressed.

Contact information for the corresponding author: Fredrik Landfors, Department of Public Health and Clinical Medicine, Umea□ University, S-901 87 Umea□, Sweden; Email: Fredrik.Landfors@umu.se; Phone: +46 (0) 70-454 92 08.

ABSTRACT

Background and Aims: APOC3, ANGPTL3, and ANGPTL4 are circulating proteins that are actively pursued as pharmacological targets to treat dyslipidemia and reduce the risk of atherosclerotic cardiovascular disease. Here, we used human genetic data to compare the predicted therapeutic and adverse effects of APOC3, ANGPTL3, and ANGPTL4 inactivation.

Methods: We conducted drug-target Mendelian randomization analyses using variants in proximity to the genes associated with circulating protein levels to compare APOC3, ANGPTL3, and ANGPTL4 as drug targets. We obtained exposure and outcome data from large-scale genome-wide association studies and used generalized least squares to correct for linkage disequilibrium-related correlation. We evaluated six primary cardiometabolic endpoints and screened for potential side effects across 694 disease-related endpoints, 43 clinical laboratory tests, and 11 internal organ MRI measurements.

Results: Genetically lowering circulating ANGPTL4 levels reduced the odds of coronary artery disease (CAD) (odds ratio, 0.57 per s.d. protein [95%CI,0.47–0.70]) and type 2 diabetes (T2D) (odds ratio, 0.73 per s.d. protein [95%CI,0.57–0.94]). Genetically lowering circulating APOC3 levels also reduced the odds of CAD (odds ratio, 0.90 per s.d. protein [95%CI,0.82–0.99]). Genetically lowered ANGPTL3 levels via common variants were not associated with CAD. However, meta-analysis of loss-of-function variants revealed that *ANGPTL3* inactivation protected against CAD (odds ratio, 0.71 per allele [95%CI,0.62–0.82]). Analysis of lowered ANGPTL3, ANGPTL4, and APOC3 levels did not identify important safety concerns.

Conclusion: Human genetic evidence suggests that therapies aimed at reducing circulating levels of ANGPTL3, ANGPTL4, and APOC3 reduce the risk of CAD. ANGPTL4 lowering may also reduce the risk of T2D.

STRUCTURED GRAPHICAL ABSTRACT

Key Question: Does human genetics support that triglyceride-lowering drugs targeting ANGPTL3, ANGPTL4, and APOC3 will reduce the risk of cardiometabolic disease without causing side effects?

Key Finding: Genetically lowered circulating ANGPTL4 reduced coronary artery disease and type 2 diabetes risk. Genetically lowered ANGPTL3 and APOC3 also reduced coronary artery disease risk, but no impact on type 2 diabetes risk was observed.

Take-home Message: Human genetics suggest that ANGPTL3, ANGPTL4, and APOC3-lowering medications may prevent CAD. Medicines targeting ANGPTL4 may have added benefits for patients with type 2 diabetes.

INTRODUCTION

APOC3, ANGPTL3, and ANGPTL4 are circulating proteins that regulate plasma cholesterol and triglyceride (TG) levels. They mainly act by inhibiting the enzyme lipoprotein lipase. All three proteins are actively pursued as pharmacological targets to treat dyslipidemia and reduce the risk of atherosclerotic cardiovascular disease. The inactivation of APOC3 using ASOs (Volanesorsen, Olezarsen) has been shown to substantially reduce plasma TG levels in different patient groups with severe hypertriglyceridemia (1). Volanesorsen is a second-generation ASO that was approved in Europe for treating familial chylomicronemia syndrome. Olezarsen is a third-generation ASO that very recently received fast-track designation from the FDA. Currently, several human trials are ongoing with an RNAi against APOC3 called ARO-APOC3.

Similar to APOC3, the inactivation of ANGPTL3 using monoclonal antibodies (Evinacumab) (2-6), antisense oligonucleotides (ASOs) (Vupanorsen) (7, 8), and RNAi (ARO-ANG3) has been shown to significantly lower plasma LDL-C and TG levels in various dyslipidemic patients groups (9). Evinacumab was approved in 2021 as a treatment for homozygous familial hypercholesterolemia (HoFH), while Vupanorsen was discontinued in 2021 due to the limited reduction in non-HDL-C and TG and increases in liver fat and enzymes (10). Recent case reports suggest that Evinacumab may promote the regression of atherosclerotic plaques in HoFH patients (11, 12).

Whereas the clinical development of anti-APOC3 and -ANGPTL3 treatments have progressed well, therapies targeting ANGPTL4 have faced delay because mice deficient in ANGPTL4 develop lethal mesenteric lymphadenopathy and chylous ascites when fed a diet high in saturated fatty acids (13-15). Whether whole-body inactivation of ANGPTL4 might trigger similar pathological features in humans is unclear. As an alternative pharmacological strategy, inactivating ANGPTL4 specifically in the liver holds considerable promise (16).

Human genetic data can be leveraged to predict the clinical effect of the pharmacological inactivation of genes or proteins. Here, we aimed to compare the predicted therapeutic effects of APOC3, ANGPTL3, and ANGPTL4 inactivation by investigating the biological and clinical impact of inactivation variants in the respective genes. In addition, to address safety concerns, we compared the predicted detrimental effects of APOC3, ANGPTL3, and ANGPTL4 inactivation on relevant disease

outcomes. We conclude that therapies specifically aimed at decreasing plasma ANGPTL3, ANGPTL4, and APOC3 levels are expected to reduce the risk of coronary artery disease without raising safety concerns. Therapies targeting ANGPTL4 levels are expected to favorably impact the risk of type 2 diabetes. This suggests that reducing ANGPTL4 could offer therapeutic advantages to a wider group of patients with dyslipidemia and type 2 diabetes.

METHODS

Study design and data sources

To estimate the causal effects of pharmacologically inactivating the *ANGPTL3*, *ANGPTL4*, and *APOC3* genes, we performed two-sample drug-target Mendelian randomization analyses (MR). We used, as instrumental variables (IV), genetic variants within 2.5 kilobase pairs (Kb) of the target gene that had genome-wide significant associations (P-value $\leq 5\times10^{-8}$) with protein abundance and plasma TG, as determined by genome-wide association studies (GWAS). Plasma protein abundance was measured in GWAS using the SomaScan and Olink platforms (17, 18). GWAS data on plasma TG, LDL cholesterol, HDL cholesterol, apolipoprotein B, apolipoprotein A1, and lipoprotein(a) were retrieved from the 2018 Neale Lab UK biobank analysis (http://www.nealelab.is/uk-biobank/). For the functional variant analyses, genetic association data on TG, LDL cholesterol, and HDL cholesterol were retrieved from the AstraZeneca UK biobank exome sequencing-based phenome-wide association study (PheWAS) portal (19). We obtained outcome summary data from GWAS of six cardiometabolic disease endpoints, 16 cardiometabolic risk markers, 43 routine clinical chemistry tests, 11 internal organ MRI measurements, and five abdominal lymphadenopathy-related phenotypes (see **Table 1**, **Supplemental Table 1,** and **Supplemental Methods**). Phenome-wide MR analyses were conducted in FinnGen and the UK biobank. FinnGen integrates genotype data from Finnish biobanks with longitudinal health registry data (20). The UK Biobank is a large-scale research resource containing genetic, blood chemistry, imaging, and health record data from half a million UK participants (21). FinnGen data freeze 10 and UK biobank meta-analysis (https://public-metaresults-fg-ukbb.finngen.fi) stores genetic association statistics on 694 disease-related outcomes from 301,552–882,347 individuals. Further details on the study design are given in the **Supplemental Methods**.

TABLE 1

Table 1. Description of GWAS data sets

	Trait	First author (year)	Consortium	Sample size (events/total)	Population
pQTL	Plasma protein abundance (SomaScan)	Ferkingstad (2021) (17)	deCODE	35,559	Icelandic
	Plasma protein abundance (Olink)	Dhindsa (2023) (18)	Not available	50,829	British
Diseases	Coronary artery disease	Aragam (2022) (22)	CARDioGRAMplus C4D; EPIC-CVD	181,522 / 1,165,690	European
	Chronic kidney disease	Wuttke (2019) (23)	CKDGen	41,395 / 480,698	European
	Ischemic stroke	Mishra (2022) (24)	GIGASTROKE	62,100 / 1,296,908	European
	Non-alcoholic fatty liver disease	Ghodsian (2021) (25)	Not available	8,434 / 787,048	European
	Type 2 diabetes; Type 2 diabetes adjusted for Body Mass Index (BMI)	Mahajan (2018) (26)	DIAGRAM	74,124 / 898,130	European
Risk factors	Plasma total, HDL, and LDL cholesterol; Apolipoprotein B; Apolipoprotein A1; TG; Lipoprotein(a); HbA1c	Neale lab (2018)	Not available	273,896 – 344,278;	British
	HDL, and LDL cholesterol; TG; NMR metabolomics	Wang (2021) (19); Nag (2023) (27)	AZPheWAS	95,077 – 376,311	British
	NMR metabolomics, including total lipoprotein phospholipids	Elsworth (2020) (30)	MRC-IEU	110,058 – 115,078	British
	Systolic blood pressure; diastolic blood pressure	Evangelou (2018) (28)	Not available	757,601	European
	BMI; waist-hip ratio (with and without adjustment for BMI)	Pulit (2018) (29)	GIANT	694,649 – 806,834	European
	Body fat percentage; NMR total triglycerides; NMR total phospholipids	Elsworth (2020) (30)	MRC-IEU	115,078 – 454,633	British
	Plasma creatinine estimated glomerular filtration rate (eGFR); cystatin C eGFR	Stanzick (2021) (31)	CKDGen	1,004,040; 1,201,909	European; 86% European
Safety-related	Magnetic resonance imaging of internal organs	Liu (2021) (32)	Not available	25,617 – 32,860	British
	Routine blood chemistry tests	Neale lab (2018)	Not available	30,565 – 350,812	British
	Acute lymphadenitis; Acute peritonitis; Ascites; Intestinal malabsorption; Non-infectious lymphatic disorders	Neale lab (2018); Kurki (2023) (20)	Not available; FinnGen	620 – 4,982 / 270,172 – 382,633; 798 – 1643 / 295,812 – 341,350	British; Finnish
	Phenome-wide association study	FinnGen (2023) (20)	Pan-UK Biobank + FinnGen meta-analysis	110 – 279,543 / 301,552 – 882,347	British; Finnish

Statistical methods

Drug-target MR analyses

In the drug-target MR analyses, we identified variants within 2.5 Kb of each gene associated (P-value $\leq 5\times10^{-8}$) with either plasma protein abundance (called *cis* protein quantitative trait loci, *cis*-pQTLs), or plasma TGs. The precision of the inverse-variance weighted (IVW) estimator can be influenced by LD-related correlation between the genetic IV in the drug target genes *cis'* position. Therefore, we used a generalized least squares (GLS) IVW MR estimator to correct for this potential source of bias (33, 34). The GLS-corrected MR approach can be conceptualized as combining the independent information of variants in the vicinity of a target gene while maintaining robust standard errors through weighting for their LD-related correlation. Variants in each target gene were clumped at an LD threshold of $r^2 \geq 0.10$ to avoid GLS-related multicollinearity issues. Further information regarding the methodology can be found in the **Supplemental Methods**.

A list of the genetic instruments used for the MR is provided in **Table 2**. Due to the complex LD structure of the *APOA1-APOA5-APOC3* locus, we supplemented the original analyses with a second model of APOC3 lowering. In this model, APOC3 lowering was instrumented through the *APOC3 c.55+1G>A* splice donor loss variant. Furthermore, we used *LPL* and genome-wide TG-associated variants as positive controls. *LPL* was analyzed using drug-target MR. For the genome-wide TG-associated variant MR, we tested the causal effect of TG using variants in chromosomes 1-22 associated with TG at P-value $\leq 5\times10^{-8}$. An LD clumping window of 500 Kb and a threshold of $r^2 \geq 0.001$ was applied before analysis using an IVW MR estimator.

TABLE 2

Table 2. Genetic instruments **Effect (P-value)**

	rsID	Variant	HGVS	Consequence	Frequency	Protein	TG
ANGPTL3	rs79151558	1:62595131:A>G		Upstream variant	0.028	-0.32 (8.1e-39)	-0.06 (5.4e-13)
	rs11207997*	1:62596235:C>T		Upstream variant	0.338	-0.22 (1.2e-144)*	-0.08 (2.7e-221)*
	rs17123728	1:62602628:G>A	c.931+248G>A	Intron variant	0.04	n.s.	0.03 (2.5e-08)
	rs35285100	1:62603486:T>C	c.932-483T>C	Intron variant	0.071	0.10 (2.3e-09)	n.s.
	rs10789117*	1:62606594:A>C		Downstream variant	0.354	-0.22 (1.7e-144)*	-0.08 (1.6e-221)*
	rs6678483*	1:62608771:C>A		Downstream variant	0.354	-0.22 (1.7e-144)*	-0.08 (2e-221)*
ANGPTL4	rs116843064	19:8364439:G>A	p.Glu40Lys	Missense variant	0.024	-0.32 (6.6e-35)	-0.21 (3.2e-127)
	rs149480839	19:8368237:C>T	c.548-982C>T	Intron variant	0.03	n.s.	-0.05 (2.6e-14)
	rs139469000	19:8376253:C>T		Downstream variant	0.28	n.s.	-0.02 (1.7e-09)
APOC3	rs2727788	11:116828247:C>A		Upstream variant	0.262	n.s.	-0.05 (7.3e-83)
	rs138326449	11:116830638:G>A	c.55+1G>A	Splice donor variant	0.002	-2.19 (3.2e-142)	-0.86 (3.4e-157)
	rs5141	11:116831407:T>C	c.179+511T>C	Intron variant	0.916	-0.17 (2.1e-38)	-0.19 (<2e-308)
	rs5132	11:116832062:C>T	c.180-702C>A	Intron variant	0.015	n.s.	0.06 (3.1e-08)
	rs12721031	11:116833789:C>T		Downstream variant	0.023	n.s.	-0.06 (2.6e-12)
	rs10750098	11:116834852:G>T		Downstream variant	0.115	-0.17 (2.1e-38)	-0.19 (<2e-308)
	rs12721028	11:116834874:A>G		Downstream variant	0.159	n.s.	0.04 (2e-35)
	rs12718462	11:116835003:T>C		Downstream variant	0.066	n.s.	-0.05 (1.8e-22)

Sensitivity analyses

Drug-target MR substantially relies on the assumption that LD (a phenomenon in which neighboring genetic variants are inherited together more frequently than anticipated by chance (35)) does not confound the association between variant and outcome. In cases where there are distinct genetic variants affecting both the exposure and the outcome, and they are connected through LD, there is a risk of making incorrect conclusions (36). To limit this issue, we performed colocalization analyses, which test whether two independent association signals in the same gene region are consistent with having a single shared causal variant (that is, testing if the association signals are 'colocalized') (37). To assess possible confounding from LD, all drug target MR analyses were complemented by colocalization analysis of the 500 Kb (±250 Kb) region surrounding each target gene (37). Further details regarding colocalization, LD matrix sensitivity, and sample overlap bias analyses are provided in the **Supplemental Methods**.

We performed sensitivity MR analyses of *ANGPTL3*, *ANGPTL4*, *APOC3*, *LPL*, and *LIPG* on CAD, by restricting the genetic instrument selection to variants within these target genes that are predicted to have functional impacts. This strategy aimed to mitigate potential biases arising from common non-coding small-effect variants outside the target genes, which could be confounded due to linkage disequilibrium with other genes in the same genomic region. Ensembl Variant Effect Predictor (VEP) version 109 (38) was used to annotate the variants within 2.5 Kb of the gene that were associated ($P \leq 0.01$) with target protein levels and any plasma lipid measurement (ApoB, ApoA-I, TG, HDL-C, or LDL-C) in (19). Non-coding variants outside of the 5' untranslated region (UTR), 3' UTR, or splice site regions were filtered out and excluded from further analysis, as were missense variants lacking SIFT deleterious or PolyPhen likely or probably damaging annotations. MR was conducted for single variants using the Wald ratio estimator, and meta-analysis was performed using a random-effects IVW estimator.

Lymphadenopathy and phenome-wide MR analyses

A Wald ratio estimator was used for the single-variant MR of lymphadenopathy-related phenotypes and the phenome-wide MR conducted in FinnGen (39). The variants were selected based on being within 2.5 Kb of the drug target gene, their strength of association with target protein plasma abundance ($P \leq 5\times10^{-8}$), their strength of association with triglyceride levels ($P \leq 5\times10^{-8}$), and their functional consequence (the same criteria as outlined above for the CAD MR limited to functional variants).

Genetic mimicry analyses

Genetic mimicry analysis was used to compare the metabolic concordance of common and rare variants in the genes *ANGPTL3*, *ANGPTL4*, and *APOC3*. This method uses linear regression to determine the extent of similarity between different variants' genetic associations in high-dimensional data sets (40, 41). The degree of concordance is given as the coefficient of determination (R^2). Genetic association effect estimates for the common variants (CVs) were derived using drug-target MR with plasma TGs as the exposure. The PTV estimates were extracted from the *ptv5pcnt* collapsing models from the Astra Zeneca PheWAS portal (27). Gene variant-metabolite association pairs with an association strength of $P \geq 0.10$ were excluded from the analyses. The collapsing model estimates were scaled by their 1-s.d. effect on plasma TGs to improve interpretability.

Meta-analysis of the impact of loss-of-function variants on CAD

We conducted a meta-analysis to assess how loss-of-function (LoF) variants in *ANGPTL3*, *ANGPTL4*, and *APOC3* impact the risk of CAD. To minimize the influence of incorrect genotype calls for rare variants, the meta-analysis was limited to studies where genotypes were determined by DNA sequencing. When multiple papers reported on individuals from overlapping cohorts or case-control studies, we selected the substudy with the largest sample size for inclusion in the meta-analysis. We determined the impact of the inactivating variants on CAD risk per mmol/L reduction of TG and per inactivating allele using fixed-effect IVW estimators. If no within-sample association of inactivating variants with TG concentrations (in mmol/L) was available, the combined IVW meta-analysis TG estimate was used as the denominator to determine the CAD odds per mmol/L TG effect. UK biobank LoF variants associated with CAD (UKB Phenotypic Release v51165: "union#I25#Chronic ischaemic heart disease") were retrieved from the Astra Zeneca PheWAS portal using the *flexdmg*, *flexdmg*, and

ptv5pcnt models for *ANGPTL3*, *ANGPTL4*, and *APOC3*, respectively (19). Statistical heterogeneity across studies was estimated by calculating the Cochran Q statistic.

Multiple testing

P-values and 95% confidence intervals (CI) are reported using analysis-type Bonferroni multiple comparisons correction. In the primary MR analyses, we corrected for the six cardiometabolic disease outcomes that were run across three different drug-target gene exposures (*ANGPTL3, ANGPTL4, APOC3*) for protein abundance, and four genes for the TG exposure (*ANGPTL3, ANGPTL4, APOC3, LPL*). Additionally, we included sixpolygenic MR models, totaling 48 multiple comparisons for the cardiometabolic disease outcomes. In the cardiometabolic risk factor MR analyses of *cis*-pQTLs, we made corrections for 48 multiple comparisons (16×3). Similarly, imaging and clinical chemistry MR analyses were corrected for 33 (11×3), and 129 (43×3) multiple comparisons, respectively. We did not perform multiple comparison corrections for the *ANGPTL4*-targeted MR analyses of the lymphadenopathy-related phenotypes. This was because identifying potential safety concerns that needed to be addressed was considered more critical than stringent multiplicity correction for these specific outcomes. Similarly, the primary motivation for performing the functional variant-limited CAD MR analyses and rare inactivating variant meta-analysis was to reduce the risk of false-negative findings. Additionally, we wanted to ensure that these CIs and P-values remained comparable across different studies. These CIs and P-values were, therefore, not corrected for multiple comparisons. The significance threshold in the phenome-wide *cis*-pQTL MR analyses was set at 2082 multiple comparisons (694 phenotypes in the FinnGen R10 and UK biobank meta-analysis, times three genes).

RESULTS

The results of the drug-target MR analyses of cardiometabolic diseases, cardiometabolic risk factors, and the safety-related endpoints are presented in **Figure 1**, **Figure 2**, and **Figure 3**, respectively. MR scatter, colocalization plots, and results tables with greater detail are provided in **Supplemental Figures 1-2** and **Supplemental Table 2**. Detailed PheWAS results are provided in **Supplemental Tables 6-9**.

Drug-target MR of cardiometabolic diseases

Genetically mediated changes in plasma ANGPTL3 protein abundance were not associated with a reduced risk of any cardiometabolic outcome (**Figure 1A**). Neither were *ANGPTL3*-mediated changes in plasma TG (**Figure 1B**). The p.E40K coding variant was the only variant that qualified as a *cis*-pQTL in the *ANGPTL4* region. *ANGPTL4* p.E40K is a common missense variant (allele freq. ~2% in Europeans) that destabilizes ANGPTL4 after secretion and prevents ANGPTL4 from inhibiting LPL (42). Changes in ANGPTL4 protein abundance via *ANGPTL4* p.E40K were associated with a decreased risk of CAD (OR: 0.57, $P=2\times10^{-19}$), T2D (OR: 0.73, P=0.002), and T2D adjusted for BMI (OR: 0.61, $P=2\times10^{-7}$) (**Figure 1A**). Similarly, changes in plasma TG levels via three *ANGPTL4* variants were associated with a decreased risk of CAD (OR: 0.43, $P=2\times10^{-21}$), T2D (OR: 0.62, $P=7\times10^{-4}$), and T2D adjusted for BMI (OR: 0.47, $P=4\times10^{-8}$) (**Figure 1B**). In addition, colocalization analyses indicated a high probability of *ANGPTL4* p.E40K being a shared causal variant for ANGPTL4 abundance and TG levels with CAD, T2D, and T2D adjusted for BMI, respectively (pp. H_4: 98–100%) (**Figures 1A-B**). Changes in APOC3 levels caused by *APOC3* variants were associated with a reduced risk of CAD (OR: 0.90, P=0.014) (**Figure 1A**), as were changes in TG levels through *APOC3* variants (OR: 0.80, $P=6\times10^{-11}$). The *APOC3* c.55+1G>A splice donor loss variant had a substantial impact on plasma APOC3 levels (-2.19 s.d. protein, $P=3.2\times10^{-142}$) (**Table 2**). When compared to the model allowing for multiple variants in the *APOC3* region, APOC3 lowering modeled through the *APOC3* c.55+1G>A variant demonstrated a comparable correlation with CAD in terms of the direction of its effect. However, the association was non-significant (**Figure 1**).

Similar to APOC3 and ANGPTL4, changes in plasma TG levels through *LPL* variants were associated with a reduced risk of CAD (OR: 0.69, $P=2\times10^{-24}$), NAFLD (OR: 0.66, P=0.03), and T2D (OR: 0.80, $P=6\times10^{-11}$) (**Figure 1B**).

Drug-target *cis*-pQTL MR of cardiometabolic risk factors

Genetically lowered plasma ANGPTL3 levels mediated through *ANGPTL3* variants were associated with reduced total cholesterol (-0.27 mmol/L, $P=2\times10^{-107}$), TG (-0.34 mmol/L, $P=6\times10^{-206}$), LDL-C (-0.15 mmol/L, $P=2\times10^{-57}$), ApoB (-0.03 g/, $P=3\times10^{-36}$), and ApoA-I levels (-0.05 g/L, $P=1\times10^{-51}$), while the effect on HDL-C was comparatively weak (-0.02 mmol/L, $P=4\times10^{-5}$) (**Figure 2**).

Genetically lowered plasma ANGPTL4 levels instrumented through the p.E40K variant were associated with reduced plasma TG (-0.65 mmol/L, $P=1\times10^{-125}$) and weakly reduced ApoB levels (-0.02 g/L, P=0.04), as well as increased ApoA1 (0.11 g/L, $P=2\times10^{-55}$) and HDL-C levels (0.24 mmol/L, $P=8\times10^{-134}$) (**Figure 2**). Genetically lowered plasma ANGPTL4 levels were also associated with modest reductions in the waist-hip ratio (-0.09 s.d., P=0.005), and the waist-hip ratio adjusted for BMI (-0.12 s.d., $P=2\times10^{-5}$), and a small increase in body fat percentage (0.07 s.d., P=0.009) (**Figure 2**).

Genetically lowered plasma APOC3 levels were associated with reduced TG levels (-0.58 mmol/L, $P < 2\times10^{-308}$) (**Figure 2**). APOC3 levels were also associated with ApoB (-0.03 g/L, $P=3\times10^{-22}$), LDL-C (-0.10 mmol/L, $P=7\times10^{-18}$), HDL-C (0.16 mmol/L, $P < 2\times10^{-238}$), and total cholesterol (-0.08 mmol/L, $P=5\times10^{-6}$) (**Figure 2**). In terms of association and effect directionality, these results closely resembled those of the *APOC3 c.55+1G>A* model (**Figure 2**).

Drug-target MR of potential adverse effects

Genetic lowering of plasma protein levels of the target genes was not associated with any of the MRI imaging endpoints (**Figure 3A**). 9, 3, 9, and 6 out of the 43 routine clinical laboratory tests showed statistically significant associations by drug-target cis-pQTL MR of the *ANGPTL3*, *ANGPTL4*, *APOC3*, and *c.55+1G>A* models, respectively (**Figure 3B**). The effect magnitudes were weak. For example, genetically lowered ANGPTL3 and APOC3 levels were significantly associated with

increased platelet count. However, the effect was estimated to be 4–5×10^9 cells/L per s.d. lowered plasma protein levels, which was minimal compared to the population mean value of 252×10^9 cells/L.

Given that safety concerns have arisen from preclinical models of ANGPTL4 deficiency, we conducted targeted cis-pQTL MR analyses of *ANGPTL4* on disease phenotypes that may be associated with abdominal lymphadenopathy. The mechanism behind the fatal chylous lymphadenopathy observed in mice was purportedly the loss of inhibition of LPL in macrophages, which caused them to take up excess lipids, leading to massive inflammation in the mesenteric lymph system (14). Exposure to *ANGPTL4* suppression was instrumented using two different models: by the ANGPTL4 p.E40K coding variant, and by the ANGPTL4 p.Cys80frameshift (fs) variant. *ANGPTL4* p.Cys80fs is a high-confidence predicted LoF variant. It is enriched in Finns compared to non-Finnish Europeans (allele frequency: 0.63% vs. 0.05%). *Cis*-pQTL MR via the relatively common *ANGPTL4* p.E40K variant was conducted at five different phenotypes that may be related to lymphadenopathy and malabsorptive states. Four had overlapping phenotype codes between the UK biobank and FinnGen and were meta-analyzed using IVW meta-analysis. ANGPTL4 levels via p.E40K were not associated with any of the five phenotypes (**Figure 3C**). However, since the confidence intervals were wide, we cannot fully exclude an association of p.E40K within this interval. Genetically lowered plasma ANGPTL4 levels via the *ANGPTL4* p.Cys80fs variant were not associated with any of the four FinnGen phenotypes that may be related to lymphadenopathy and malabsorptive states (**Figure 3C**).

To investigate if there was any genetic evidence for unknown ANGPTL4-mediated side effects, we performed cis-pQTL MR on 694 disease-related phenotypes in FinnGen and the UK Biobank via the *ANGPTL4* p.E40K and p.Cys80fs variants. Using a phenome-wide significance threshold of $P \leq \frac{0.05}{3\times694}$, we found no evidence for increased risk of any endpoint via p.E40K- or p.Cys80fs-lowered ANGPTL4 levels (**Figure 3D**). Instead, we found phenome-wide evidence that p.E40K reduced the risk of four CAD-related phenotypes, including myocardial infarction and one T2D-related phenotype, while also being associated with a lowered probability of statin prescription, lipoprotein disorders, and hypercholesterolemia (**Figure 3D**). Additionally, *ANGPTL4* p.Cys80fs was associated with a

decreased risk of two T2D-related outcomes and a lowered probability of statin prescription and hypercholesterolemia diagnosis (**Figure 3D**).

The phenome-wide MR results of lowered plasma ANGPTL4 levels were compared with ANGPTL3 and APOC3 by cis-pQTL MR of the 694 FinnGen and UK Biobank endpoints using the *ANGPTL3* c.*52_*60del and *APOC3* c.55+1G>A. Genetically lowered plasma ANGPTL3 levels were associated with a reduced risk of being prescribed statin medication, two lipid-related diagnosis codes but not any other patient-related outcome (**Supplemental Figure 3A**). *APOC3 c.55+1G>A* was associated with a reduced risk of statin prescription but not any other endpoint (**Supplemental Figure 3B**).

Common variants in *ANGPTL3*, *ANGPTL4*, and *APOC3* share their metabolic fingerprint with loss-of-function variants

In line with a previous investigation (43), we found no significant association between *ANGPTL3* suppression via common variants and CAD. Previously, however, evidence was presented that loss-of-function variants in *ANGPTL3* are associated with a decreased risk of CAD (44, 45). As the common variants in *ANGPTL3* presented here only modestly impacted plasma lipids, it could be argued that they do not accurately reflect the effects of more profound *ANGPTL3* suppression. Therefore, we examined whether common variants in *ANGPTL3*, *ANGPTL4*, and *APOC3* mimicked the effects (that is, showed the same effect directionality) of more deleterious protein-truncating variants (PTVs). PTVs often result in protein loss-of-function and, accordingly, are powerful genetic instruments to study the potential impact of pharmacological gene silencing (46).

All common variants in *ANGPTL3*, *ANGPTL4*, and *APOC3* were highly concordant with PTVs within the same gene (**Figure 4A-C**). One hundred thirty-seven metabolite associations in *ANGPTL3* showed a high concordance metric (R^2) of 85% between the common variants and PTV models. *ANGPTL4* common variants were also highly concordant with *ANGPTL4* PTVs, having an R^2 of 89% for a set of 86 metabolites, while *APOC3* showed a concordance metric R^2 of 91% in 137 metabolic parameters. These results demonstrate that the common genetic variations in *ANGPTL3*, *ANGPTL4*, and *APOC3* would be valid genetic instruments reflecting a modest “knock-down” of each respective gene.

Comparative drug-target MR of LPL and endothelial lipase (EL) reveals that in order to achieve CAD benefits, ANGPTL3 inhibition should primarily target LPL rather than EL

ANGPTL3 targets both EL and LPL and may thus influence CAD via two independent pathways (47). To compare the effects of these two target enzymes, we analyzed the effects of genetically instrumented EL and LPL activity on CAD by performing functional-variant limited MR of the *LIPG* (encoding EL) and *LPL* genes. We used the preferred enzyme substrate as the exposure, using plasma lipoprotein phospholipids for EL and total plasma TGs for LPL. We detected two functional *LPL* variants and four functional *LIPG* variants that had small to large effects on plasma TG/lipoprotein phospholipids (range: 0.02 – 0.6 s.d. per allele). Allele frequencies and imputation quality ('INFO' score) are given in **Figure 4D**.

MR analysis of *LPL* and *LIPG* found opposing significant associations for LPL (IVW meta-analysis: OR: 0.74, $P=1\times10^{-4}$) and EL (IVW meta-analysis OR: 1.38, $P=5\times10^{-7}$) (**Figure 4D**). These findings suggest that increased activity of LPL protects against the development of atherosclerosis, whereas heightened activity of EL may contribute to the acceleration of atherosclerosis. The contrasting impact of genetic EL and LPL activity on the risk of CAD suggests that in order to provide any net decrease in CAD risk, *ANGPTL3* inactivation may have to profoundly impact LPL activity more than EL activity.

Loss-of-function variants in *ANGPTL3, ANGPTL4,* and *APOC3,* and the risk of CAD

Two previous exome-sequencing studies found LoF variants in *ANGPTL3* to be protective of CAD (3, 44). In an effort to reproduce these findings, we performed a sensitivity MR analysis of CAD and limited the selection of genetic instruments to functional variants. Functional annotations were detected for five *ANGPTL3*, two *ANGPTL4*, and one *APOC3* variant. The detected *APOC3* variant was the *c.55+1G>A* splice donor loss variant, which was already reported in **Figures 1-3**. The other variants lowered protein abundance, with impact sizes ranging from profound to modest (range: -2.53– -0.28) (**Figure 4E**) (18). The variants were analyzed individually and together using random-effects IVW meta-analysis. *Cis*-pQTL MR of the *ANGPTL3* variants indicated that ANGPTL3 protein levels were not significantly associated with CAD, either individuallyor together (meta-analysis IVW OR:

0.98, P=0.13) (**Figure 4E**). By contrast, reduced *ANGPTL4* protein levels were associated with a decreased risk of CAD (meta-analysis IVW OR: 0.67, P=0.007) (**Figure 4E**).

Considering the beneficial effects of ANGPTL3, ANGPTL4, and APOC3 on plasma lipids, it was expected that genetic inactivation of these genes would confer protection against CAD. However, the MR analyses focusing on common variants of *ANGPTL3*, as well as MR of functional variants (both rare and common, identified through DNA microarray technology), did not support this hypothesis. Therefore, we pursued a meta-analysis of DNA sequencing-based studies that studied the effect of *ANGPTL3*, *ANGPTL4*, and *APOC3* LoF variants on CAD. The rationale for excluding DNA microarray and exome bead chip-based studies was that they could potentially introduce measurement error for rare variants (48, 49). This would lead to bias towards the null hypothesis. DNA-sequencing-based substudies from previous papers (3, 44, 50, 51), were extracted and analyzed together with the chronic ischemic heart disease case-control subset in the UK biobank (19). The total number of individuals included in the meta-analysis amounted to 372,837 for *ANGPTL3*, 189,672 for *ANGPTL4*, and 160,230 for *APOC3*. The carrier status of LoF variants was associated with substantial decreases in protein levels for both *ANGPTL3* (-1.73 s.d. protein, $P=3.2\times10^{-121}$) and *ANGPTL4* (-1.65 s.d. protein, $P=1.5\times10^{-102}$). APOC3 protein levels were not measured in the UK Biobank. However, *APOC3* LoF variants were associated with a significant reduction in TG levels (**Figure 5**).

The results of the meta-analysis are presented in **Figure 5**. The presence of *ANGPTL3* LoF variants was associated with reduced CAD risk (meta-analysis IVW OR: 0.45 per TG, $P=5.3\times10^{-7}$). *ANGPTL4* LoF variant carrier status, excluding p.E40K, was also associated with a reduced risk of CAD (meta-analysis IVW OR: 0.35 per TG, P=0.017), as was *APOC3* LoF variant carriers status (meta-analysis IVW OR: 0.80 per TG, P=0.021). The key finding was the robust association of *ANGPTL3* LoF carrier status with a reduced risk of CAD. This association was not detected by the other approaches and implies that ANGPTL3 lowering might offer similar atheroprotective benefits comparable to those achieved by ANGPTL4 or APOC3 lowering.

DISCUSSION

We find that targeted inactivation and associated lowering of plasma APOC3 levels is predicted to decrease plasma TG and LDL and raise HDL levels. Targeted lowering of plasma ANGPTL3 is expected to reduce plasma TG, LDL, and HDL levels, while lowering of plasma ANGPTL4 is predicted to decrease plasma TG and increase HDL levels. Based on these findings, it is expected that genetic inactivation of APOC3, ANGPTL3, and ANGPTL4 levels is associated with protection against CAD. Through MR and a meta-analysis of rare variant genetic association studies, we confirmed that targeted inactivation and lowering of ANGPTL3, ANGPTL4, and APOC3 is associated with a lowered risk of CAD. In addition, lifetime genetic lowering of ANGPTL4 was observed to reduce the risk of T2D, indicating that ANGPTL4 inhibition might provide additional benefits to patients with T2D and dyslipidemia.

The inactivation of ANGPTL4 in mice and monkeys was shown to lead to mesenteric lymphadenopathy and other severe complications. Naturally, these observations raised serious concerns about the safety of pharmacological targeting of ANGPTL4. Here, we did not find an association between genetic ANGPTL4 inactivation and several disease codes related to lymphatic disorders. While these data do not entirely exclude any harmful effects of ANGPTL4 inactivation, they do mitigate safety concerns about the impact of whole-body inactivation of ANGPTL4 in humans. Recently, it was shown that silencing of ANGPTL4 in the liver and adipose tissue using ASO markedly reduces plasma TG levels in mice yet does not lead to mesenteric lymphadenopathy or other complications (16). These data suggest that liver- and adipose tissue-specific inactivation of ANGPTL4 may confer similar cardiovascular benefits as whole-body ANGPTL4 inactivation without any particular safety risks.

Previous studies reported conflicting findings regarding the association between ANGPTL3 and CAD. Dewey et al. (3), and Stitziel et al. (44) found that rare LoF *ANGPTL3* variants were associated with decreased odds of ASCVD, whereas MR studies of common ANGPTL3-lowering variants reported negative findings (43). By meta-analysis of rare LoF variant genetic association studies, we found clear, statistically robust evidence that lifetime genetic inactivation of ANGPTL3 confers protection

against CAD. These findings are in line with recent case reports indicating that ANGPTL3 lowering with Evinacumab protects against atherosclerosis progression in HoFH patients (11, 12).

The discrepancy between the rare LoF and common variant studies of ANGPTL3's association with CAD could be due to a range of different factors. One possible explanation is the pleiotropic effects of ANGPTL3. Besides inhibiting LPL, ANGPTL3 inhibits endothelial lipase (EL) (52). In a recent paper, we showed that the LPL-independent effects of ANGPTL3 inactivation on plasma metabolic parameters showed a striking inverse resemblance with EL inactivation, suggesting that ANGPTL3 modulates plasma lipid levels by inhibiting LPL and EL (40). Here, using MR, we compared the effects of genetically instrumented EL and LPL activity on CAD. Whereas increased LPL activity reduced the odds of CAD, increased EL activity increased the odds of CAD. The observed link between EL and CAD is consistent with previous human genetic studies showing the possible harmful effects of a genetically predicted increase in EL activity (53, 54). This suggests that ANGPTL3's interaction with EL might counteract its cardiovascular benefits achieved through LPL inhibition under certain physiological conditions. While our research demonstrated metabolic concordance between ANGPTL3 common variants and LoF variants, it remains possible that more profound ANGPTL3 inactivation by LoF variants could tip the balance in favor of LPL inhibition over EL. This shift could potentially enhance the anti-atherosclerotic benefits of ANGPTL3 lowering.

Interestingly, the association of ANGPTL3 inactivation with CAD was only present for rare LoF variants when the carrier status was determined by DNA sequencing. This exposes the limitations of drug-target MR studies using DNA micro-array-based GWAS. When rare variants are incorrectly imputed, this typically introduces a one-sided loss of information that biases toward the null hypothesis, leading to falsely negative findings (49). Even though the imputation quality score (e.g., 'INFO') reports an imputation quality metric, this metric does not really measure the true imputation accuracy (57). The imputation accuracy can only truly be determined if variant carrier status is called by genotyping (e.g., via DNA sequencing). However, studying rare variants in genetic association studies is not without drawbacks. An important limitation of the use of rare variants is statistical imprecision simply due to their rarity (55). Rare variants also often emerged relatively recently and consequently are more susceptible to confounding by enrichment in specific geographical regions,

families, or socioeconomic strata (56). Even if appropriate model adjustments are applied, subtle differences in population structure could cause a small number of extra alleles to be present in the control (or case) group. This can lead to biased estimates when the rare alternative allele is present in ten, or hundred individuals in total, which is often the case for rare variant studies even when the total sample size is above hundreds of thousands. Overall, our findings underscore the importance of combining evidence from exome sequencing and common variants in genetic association studies of complex disease phenotypes.

Compared to clinical trials, MR analysis can exaggerate the magnitude of the effect of inactivating a gene/protein (58). This is because MR and other genetic association studies estimate lifelong exposure to changed gene function, while drug trials typically last 2–5 years in late adulthood. If the treatment effect multiplicatively interacts with time, MR may exaggerate it. This constraint should be considered when translating MR findings to predict the results of clinical trials. For ANGPTL4, Dewey et al. (50), found that the TG levels of p.E40K homozygotes were reduced by 0.58 mmol/L (0.92 mmol/L for p.E40K homozygotes vs. 1.49 mmol/L in non-carriers; relative change -39%) in a normotriglyceridemic population. When translating these findings (TG reduction of 0.58 mmol/L) onto the effect size on CAD found in this study, one would expect that lifetime *ANGPTL4* inactivation—in a population of normotriglyceridemic individuals—results in a risk reduction corresponding to a CAD odds ratio of 0.61 (95% CI: 0.52–0.72).

In conclusion, our genetic analysis predicts that in a broader dyslipidemic patient population, therapies aimed at decreasing plasma ANGPTL3, ANGPTL4, or APOC3 levels will be effective in preventing CAD without raising specific safety concerns. In addition, therapies aimed at reducing plasma levels of ANGPTL4 may provide additional benefits to patients with dyslipidemia and T2D.

ETHICAL REVIEW

This study analyzed scientific data that is available to the public, as detailed in **Table 1** and **Supplemental Table 1**, where references to the specific datasets can be found. Ethical oversight was conducted by review boards, ensuring that all studies complied with the ethical standards outlined in the Helsinki Declaration.

ACKNOWLEDGEMENTS

We would like to thank the participants and researchers of the CARDIoGRAMplusC4D, CKDGen, deCODE, DIAGRAM, EPIC-CVD, FinnGen, GIGASTROKE, GLGC, and UK biobank studies, as well as the other non-consortium studies.

FUNDING

This research received no specific grants from public or non-profit funding agencies.

CONFLICT OF INTEREST

F.L. is a part-time employee of Lipigon Pharmaceuticals AB. S.K.N. is the chief executive officer of Lipigon. S.K. is a paid consultant for Lipigon.

DATA AVAILABILITY STATEMENT

Database identifiers and links to the data sets are provided in **Supplemental Table 1**. The analyses in this manuscript were performed using the R programming language (v.4.2.1) with the packages coloc, cowplot, data.table, ggplot2, ggthemes, mungegwas, phewas, twosamplemr, wesanderson, writexl, and the Python programming language (v.3.8.16) using the packages numpy, pandas, and scipy. The LD matrix estimates were calculated using PLINK (v1.90b6.24).

REFERENCES

1. Tardif JC, Karwatowska-Prokopczuk E, Amour ES, Ballantyne CM, Shapiro MD, Moriarty PM, et al. Apolipoprotein C-III reduction in subjects with moderate hypertriglyceridaemia and at high cardiovascular risk. Eur Heart J. 2022;43(14):1401-12.
2. Ahmad Z, Banerjee P, Hamon S, Chan KC, Bouzelmat A, Sasiela WJ, et al. Inhibition of Angiopoietin-Like Protein 3 With a Monoclonal Antibody Reduces Triglycerides in Hypertriglyceridemia. Circulation. 2019;140(6):470-86.
3. Dewey FE, Gusarova V, Dunbar RL, O'Dushlaine C, Schurmann C, Gottesman O, et al. Genetic and Pharmacologic Inactivation of ANGPTL3 and Cardiovascular Disease. N Engl J Med. 2017;377(3):211-21.
4. Gaudet D, Gipe DA, Pordy R, Ahmad Z, Cuchel M, Shah PK, et al. ANGPTL3 Inhibition in Homozygous Familial Hypercholesterolemia. N Engl J Med. 2017;377(3):296-7.
5. Raal FJ, Rosenson RS, Reeskamp LF, Hovingh GK, Kastelein JJP, Rubba P, et al. Evinacumab for Homozygous Familial Hypercholesterolemia. N Engl J Med. 2020;383(8):711-20.
6. Rosenson RS, Burgess LJ, Ebenbichler CF, Baum SJ, Stroes ESG, Ali S, et al. Evinacumab in Patients with Refractory Hypercholesterolemia. N Engl J Med. 2020;383(24):2307-19.
7. Gaudet D, Karwatowska-Prokopczuk E, Baum SJ, Hurh E, Kingsbury J, Bartlett VJ, et al. Vupanorsen, an N-acetyl galactosamine-conjugated antisense drug to ANGPTL3 mRNA, lowers triglycerides and atherogenic lipoproteins in patients with diabetes, hepatic steatosis, and hypertriglyceridaemia. Eur Heart J. 2020;41(40):3936-45.
8. Graham MJ, Lee RG, Brandt TA, Tai LJ, Fu W, Peralta R, et al. Cardiovascular and Metabolic Effects of ANGPTL3 Antisense Oligonucleotides. N Engl J Med. 2017;377(3):222-32.
9. Watts GF, Schwabe C, Scott R, Gladding P, Sullivan D, Baker J, et al. Abstract 15751: Pharmacodynamic Effect of ARO-ANG3, an Investigational RNA Interference Targeting Hepatic Angiopoietin-like Protein 3, in Patients With Hypercholesterolemia. Circulation. 2020;142(Suppl_3):A15751-A.
10. Bergmark BA, Marston NA, Bramson CR, Curto M, Ramos V, Jevne A, et al. Effect of Vupanorsen on Non-High-Density Lipoprotein Cholesterol Levels in Statin-Treated Patients With Elevated Cholesterol: TRANSLATE-TIMI 70. Circulation. 2022;145(18):1377-86.
11. Reeskamp LF, Nurmohamed NS, Bom MJ, Planken RN, Driessen RS, van Diemen PA, et al. Marked plaque regression in homozygous familial hypercholesterolemia. Atherosclerosis. 2021;327:13-7.
12. Khoury E, Lauzière A, Raal FJ, Mancini J, Gaudet D. Atherosclerotic plaque regression in homozygous familial hypercholesterolaemia: a case report of a long-term lipid-lowering therapy involving LDL-receptor-independent mechanisms. Eur Heart J Case Rep. 2023;7(1):ytad029.
13. Desai U, Lee EC, Chung K, Gao C, Gay J, Key B, et al. Lipid-lowering effects of anti-angiopoietin-like 4 antibody recapitulate the lipid phenotype found in angiopoietin-like 4 knockout mice. Proc Natl Acad Sci U S A. 2007;104(28):11766-71.
14. Lichtenstein L, Mattijssen F, de Wit NJ, Georgiadi A, Hooiveld GJ, van der Meer R, et al. Angptl4 protects against severe proinflammatory effects of saturated fat by inhibiting fatty acid uptake into mesenteric lymph node macrophages. Cell Metab. 2010;12(6):580-92.
15. Oteng AB, Bhattacharya A, Brodesser S, Qi L, Tan NS, Kersten S. Feeding Angptl4-/- mice trans fat promotes foam cell formation in mesenteric lymph nodes without leading to ascites. J Lipid Res. 2017;58(6):1100-13.
16. Deng M, Kutrolli E, Sadewasser A, Michel S, Joibari MM, Jaschinski F, et al. ANGPTL4 silencing via antisense oligonucleotides reduces plasma triglycerides and glucose in mice without causing lymphadenopathy. J Lipid Res. 2022;63(7):100237.
17. Ferkingstad E, Sulem P, Atlason BA, Sveinbjornsson G, Magnusson MI, Styrmisdottir EL, et al. Large-scale integration of the plasma proteome with genetics and disease. Nat Genet. 2021;53(12):1712-21.
18. Dhindsa RS, Burren OS, Sun BB, Prins BP, Matelska D, Wheeler E, et al. Rare variant associations with plasma protein levels in the UK Biobank. Nature. 2023;622(7982):339-47.
19. Wang Q, Dhindsa RS, Carss K, Harper AR, Nag A, Tachmazidou I, et al. Rare variant contribution to human disease in 281,104 UK Biobank exomes. Nature. 2021;597(7877):527-32.

20. Kurki MI, Karjalainen J, Palta P, Sipilä TP, Kristiansson K, Donner KM, et al. FinnGen provides genetic insights from a well-phenotyped isolated population. Nature. 2023;613(7944):508-18.
21. Sudlow C, Gallacher J, Allen N, Beral V, Burton P, Danesh J, et al. UK biobank: an open access resource for identifying the causes of a wide range of complex diseases of middle and old age. PLoS Med. 2015;12(3):e1001779.
22. Aragam KG, Jiang T, Goel A, Kanoni S, Wolford BN, Atri DS, et al. Discovery and systematic characterization of risk variants and genes for coronary artery disease in over a million participants. Nat Genet. 2022;54(12):1803-15.
23. Wuttke M, Li Y, Li M, Sieber KB, Feitosa MF, Gorski M, et al. A catalog of genetic loci associated with kidney function from analyses of a million individuals. Nat Genet. 2019;51(6):957-72.
24. Mishra A, Malik R, Hachiya T, Jürgenson T, Namba S, Posner DC, et al. Stroke genetics informs drug discovery and risk prediction across ancestries. Nature. 2022;611(7934):115-23.
25. Ghodsian N, Abner E, Emdin CA, Gobeil É, Taba N, Haas ME, et al. Electronic health record-based genome-wide meta-analysis provides insights on the genetic architecture of non-alcoholic fatty liver disease. Cell Rep Med. 2021;2(11):100437.
26. Mahajan A, Taliun D, Thurner M, Robertson NR, Torres JM, Rayner NW, et al. Fine-mapping type 2 diabetes loci to single-variant resolution using high-density imputation and islet-specific epigenome maps. Nat Genet. 2018;50(11):1505-13.
27. Nag A, Dhindsa RS, Middleton L, Jiang X, Vitsios D, Wigmore E, et al. Effects of protein-coding variants on blood metabolite measurements and clinical biomarkers in the UK Biobank. Am J Hum Genet. 2023;110(3):487-98.
28. Evangelou E, Warren HR, Mosen-Ansorena D, Mifsud B, Pazoki R, Gao H, et al. Genetic analysis of over 1 million people identifies 535 new loci associated with blood pressure traits. Nat Genet. 2018;50(10):1412-25.
29. Pulit SL, Stoneman C, Morris AP, Wood AR, Glastonbury CA, Tyrrell J, et al. Meta-analysis of genome-wide association studies for body fat distribution in 694 649 individuals of European ancestry. Hum Mol Genet. 2019;28(1):166-74.
30. Elsworth B, Lyon M, Alexander T, Liu Y, Matthews P, Hallett J, et al. The MRC IEU OpenGWAS data infrastructure. bioRxiv. 2020:2020.08.10.244293.
31. Stanzick KJ, Li Y, Schlosser P, Gorski M, Wuttke M, Thomas LF, et al. Discovery and prioritization of variants and genes for kidney function in >1.2 million individuals. Nat Commun. 2021;12(1):4350.
32. Liu Y, Basty N, Whitcher B, Bell JD, Sorokin EP, van Bruggen N, et al. Genetic architecture of 11 organ traits derived from abdominal MRI using deep learning. Elife. 2021;10.
33. Burgess S, Dudbridge F, Thompson SG. Combining information on multiple instrumental variables in Mendelian randomization: comparison of allele score and summarized data methods. Stat Med. 2016;35(11):1880-906.
34. Schmidt AF, Finan C, Gordillo-Marañón M, Asselbergs FW, Freitag DF, Patel RS, et al. Genetic drug target validation using Mendelian randomisation. Nat Commun. 2020;11(1):3255.
35. Slatkin M. Linkage disequilibrium--understanding the evolutionary past and mapping the medical future. Nat Rev Genet. 2008;9(6):477-85.
36. Zuber V, Grinberg NF, Gill D, Manipur I, Slob EAW, Patel A, et al. Combining evidence from Mendelian randomization and colocalization: Review and comparison of approaches. Am J Hum Genet. 2022;109(5):767-82.
37. Giambartolomei C, Vukcevic D, Schadt EE, Franke L, Hingorani AD, Wallace C, et al. Bayesian test for colocalisation between pairs of genetic association studies using summary statistics. PLoS Genet. 2014;10(5):e1004383.
38. McLaren W, Gil L, Hunt SE, Riat HS, Ritchie GR, Thormann A, et al. The Ensembl Variant Effect Predictor. Genome Biol. 2016;17(1):122.
39. Abraham W. The Fitting of Straight Lines if Both Variables are Subject to Error. The Annals of Mathematical Statistics. 1940;11(3):284-300.

40. Landfors F, Chorell E, Kersten S. Genetic Mimicry Analysis Reveals the Specific Lipases Targeted by the ANGPTL3-ANGPTL8 Complex and ANGPTL4. J Lipid Res. 2023;64(1):100313.
41. Wang Q, Oliver-Williams C, Raitakari OT, Viikari J, Lehtimaki T, Kahonen M, et al. Metabolic profiling of angiopoietin-like protein 3 and 4 inhibition: a drug-target Mendelian randomization analysis. Eur Heart J. 2021;42(12):1160-9.
42. Yin W, Romeo S, Chang S, Grishin NV, Hobbs HH, Cohen JC. Genetic variation in ANGPTL4 provides insights into protein processing and function. J Biol Chem. 2009;284(19):13213-22.
43. Richardson TG, Leyden GM, Wang Q, Bell JA, Elsworth B, Davey Smith G, et al. Characterising metabolomic signatures of lipid-modifying therapies through drug target mendelian randomisation. PLoS Biol. 2022;20(2):e3001547.
44. Stitziel NO, Khera AV, Wang X, Bierhals AJ, Vourakis AC, Sperry AE, et al. ANGPTL3 Deficiency and Protection Against Coronary Artery Disease. J Am Coll Cardiol. 2017;69(16):2054-63.
45. Musunuru K, Pirruccello JP, Do R, Peloso GM, Guiducci C, Sougnez C, et al. Exome sequencing, ANGPTL3 mutations, and familial combined hypolipidemia. N Engl J Med. 2010;363(23):2220-7.
46. Rivas MA, Pirinen M, Conrad DF, Lek M, Tsang EK, Karczewski KJ, et al. Human genomics. Effect of predicted protein-truncating genetic variants on the human transcriptome. Science. 2015;348(6235):666-9.
47. Kovrov O, Kristensen KK, Larsson E, Ploug M, Olivecrona G. On the mechanism of angiopoietin-like protein 8 for control of lipoprotein lipase activity. J Lipid Res. 2019;60(4):783-93.
48. Cherukuri PF, Soe MM, Condon DE, Bartaria S, Meis K, Gu S, et al. Establishing analytical validity of BeadChip array genotype data by comparison to whole-genome sequence and standard benchmark datasets. BMC Med Genomics. 2022;15(1):56.
49. Stahl K, Gola D, König IR. Assessment of Imputation Quality: Comparison of Phasing and Imputation Algorithms in Real Data. Front Genet. 2021;12:724037.
50. Dewey FE, Gusarova V, O'Dushlaine C, Gottesman O, Trejos J, Hunt C, et al. Inactivating Variants in ANGPTL4 and Risk of Coronary Artery Disease. N Engl J Med. 2016;374(12):1123-33.
51. Jorgensen AB, Frikke-Schmidt R, Nordestgaard BG, Tybjaerg-Hansen A. Loss-of-function mutations in APOC3 and risk of ischemic vascular disease. N Engl J Med. 2014;371(1):32-41.
52. Gusarova V, Alexa CA, Wang Y, Rafique A, Kim JH, Buckler D, et al. ANGPTL3 blockade with a human monoclonal antibody reduces plasma lipids in dyslipidemic mice and monkeys. J Lipid Res. 2015;56(7):1308-17.
53. Thomas DG, Wei Y, Tall AR. Lipid and metabolic syndrome traits in coronary artery disease: a Mendelian randomization study. J Lipid Res. 2021;62:100044.
54. Singaraja RR, Sivapalaratnam S, Hovingh K, Dubé MP, Castro-Perez J, Collins HL, et al. The impact of partial and complete loss-of-function mutations in endothelial lipase on high-density lipoprotein levels and functionality in humans. Circ Cardiovasc Genet. 2013;6(1):54-62.
55. Zuk O, Schaffner SF, Samocha K, Do R, Hechter E, Kathiresan S, et al. Searching for missing heritability: designing rare variant association studies. Proc Natl Acad Sci U S A. 2014;111(4):E455-64.
56. Locke AE, Steinberg KM, Chiang CWK, Service SK, Havulinna AS, Stell L, et al. Exome sequencing of Finnish isolates enhances rare-variant association power. Nature. 2019;572(7769):323-8.
57. Zheng HF, Rong JJ, Liu M, Han F, Zhang XW, Richards JB, et al. Performance of genotype imputation for low frequency and rare variants from the 1000 genomes. PLoS One. 2015;10(1):e0116487.
58. Burgess S, Butterworth A, Malarstig A, Thompson SG. Use of Mendelian randomisation to assess potential benefit of clinical intervention. BMJ. 2012;345:e7325.

FIGURES

Graphical abstract summarizing the study's methodology and findings.

A: Graphical abstract summarizing the overall study design. **B:** A summary of the results categorized into three groups. The term 'improves' denotes a statistically significant association with a clinically relevant effect magnitude. The term 'weak' refers to a statistically significant association with no clinically significant effect. 'ASCVD' denotes atherosclerotic cardiovascular disease. 'T2D' denotes type 2 diabetes.

Figure 1. Results of MR analyses of cardiometabolic disease outcomes.

A: Forest plot and table of the *cis*-pQTL-based MR analyses. 'Events/total' indicates the outcome study's case count and total sample size. 'No. SNPS' specifies the number of variants included in the MR model. Zero SNPs indicate that none of the genetic instruments were detected in the outcome data set. 'Coloc.' shows the colocalization hypothesis ($H_{0\text{-}4}$) with the highest posterior probability (see the 'Methods' section for details about their interpretation). **B:** Results of the MR analysis using TG levels as the exposure.

Figure 2. Results of MR analyses of cardiometabolic disease risk factors.

The results are presented as bar plots, showing the magnitude of the effect per s.d. lowered protein abundance. The red lines indicate the 95 % CI. The results from cis-pQTL MR of the estimated glomerular filtration rate (eGFR) by Cystatin C and plasma Creatinine, respectively, are given in **Supplemental Figure 3**.

Figure 3. Results of MR analysis of potential adverse effects.

A: *Cis*-pQTL MR results on the imaging outcomes. Bar plots and red lines indicate the effect and 95% CI:s. 'scWAT' indicates subcutaneous white adipose tissue. 'vol.' indicates volume. **B:** *Cis*-pQTL MR of the clinical laboratory outcomes. The red bars indicate the 95 % CI. The black dots indicate the effect point estimate. '*' indicate $P < 0.05$. '**' indicates $P < 0.05$ with a shared causal variant (H_4). A list explaining the abbreviations is provided in the supplemental material (**Table S1**). **C:** Results of ANGPTL4 *cis*-pQTL MR of mesenteric lymphadenopathy and malabsorption-related phenotypes. **D:** Volcano diagram displaying the results of ANGPTL4 *cis*-pQTL phenome-wide MR scans on 694

outcomes in the FinnGen and UK Biobank meta-analysis. The *y*-axis solid straight lines indicate the phenome-wide significance threshold.

Figure 4. Results of sensitivity analyses.

The concordance between the effect directionality of CVs and PTVs is displayed using scatter plots with a regression line. **A:** Comparison of the effect directionality between *ANGPTL3* CVs and PTVs. **B:** *ANGPTL4* CVs vs. PTVs. **C:** *APOC3* CVs vs. PTVs. 'R^2' represents the coefficient of determination. 'Int.' indicates the regression line intercept. The color of the scattered dots indicates the lipid class of the NMR parameter. **D:** Forest plots and tables showing the results of the CAD MR analysis focusing on functional variants in *LPL* and *LIPG*. Genetic association summary statistics of *LIPG* with the exposure were extracted from the UK biobank NMR study of 115,078 individuals retrieved from (30). *LPL* variant associations were retrieved from the same data set. CAD data was from the Aragam et al. meta-analysis (22). **E:** Forest plots and tables showing the results of the CAD MR analysis that limited the selection of genetic instruments to functional variants in *ANGPTL3* and *ANGPTL4*. "Freq." represents the frequency of the alternative allele. "info" represents the imputation quality metric derived from the outcome GWAS. Variant effects on plasma lipids were retrieved from (19). The *ANGPTL4* p.Glu40Lys (p.E40K) estimates differ slightly from *Figure 1* because the plasma protein abundance was determined using a different method (Olink (18), instead of SomaScan (17)). There was significant heterogeneity for the ANGPTL4 IVW estimate (Cochran's Q: 11.54, P-value: 0.00068), which likely was a consequence of the *ANGPTL4* p.Arg336Cys coding variant disproportionally affecting TG levels, compared to the *ANGPTL4* p.E40K coding variant. This was supported by the fact that CAD MR by *ANGPTL4* variants using TG levels as the exposure found no significant heterogeneity (Cochran's Q: 2.3, P-value: 0.13) (**Supplemental Figure 5**).

Figure 5. Meta-analysis of loss-of-function variants in ANGPTL3, ANGPTL4, and APOC3, and the risk of CAD.

Forest plots and tables indicating the effect on CAD per TG, and per allele. The loss-of-function variant effect estimates for each substudy were retrieved from (3, 19, 44, 50, 51). The case definition used in the Copenhagen City Heart Study was not exclusively restricted to CAD. 21% of the ischemic vascular disease cases were diagnosed with atherosclerotic cerebrovascular disease, rather than CAD,

which encompassed 79 % of the cases (51). ‘Afr.’ indicates African ancestry. 'Eas.’ indicates East Asian ancestry. ‘Eur.’ denotes European ancestry. 'Sas.’ denotes South Asian ancestry.

TABLES

Table 1. Description of GWAS data sets

'NMR' indicates nuclear magnetic resonance spectroscopy.

Table 2. Genetic instruments

The genetic variants that were selected for inclusion as instrumental variables in one or more of the MR analyses whose results are shown in **Figures 1-3**. The specific instruments used in each separate MR analysis are provided in **Supplemental Table 2**. Variant consequences were retrieved from the Ensembl Variant Effect Predictor (version 109) (38). 'Effect' indicates the 1 s.d. protein abundance (retrieved from (17)) or mmol/L TG change (retrieved from http://www.nealelab.is/uk-biobank/) per allele. 'rsID' denotes Reference single nucleotide polymorphism ID. 'HGSV' indicates Human Genome Structural Variation Consortium nomenclature for sequence variants.

* These three variants were in strong linkage disequilibrium (LD) and, therefore, showed the same associations with TG levels and plasma ANGPTL3 abundance. Because they were in strong LD, they were never included in the same MR model (see **Supplemental Table 2**).

APPENDICES

Supplemental Note

In-depth information regarding diagnostic criteria for diseases, definitions of continuous outcomes, and sensitivity analyses. The supplemental note .docx also contains Supplemental Figures 1-5.

Supplemental Figures

The Supplemental Figures 1-5 are contained within the supplemental note .docx file.

Figure S1. Scatter plots showing the results of the drug-target MR analyses.

Each subplot represents the results of the analyses displayed in **Figures 1-3** of the main manuscript.

Figure S2. Regional genetic association plots displaying the results of the colocalization analyses.

Each subplot represents the results of the analyses displayed in **Figures 1-3** of the main manuscript.

Figure S3. Results of cis-pQTL MR analyses of the estimated glomerular filtration rate by (eGFR) by Cystatin C and plasma Creatinine.

The findings are displayed in bar graphs, showing the effect per s.d. decrease in protein abundance. The red lines represent the 95% CI.

Figure S4. Results of phenome-wide MR analysis on FinnGen outcomes using ANGPTL3 rs34483103-1:62604866:AGTTAATGTG>A [3 prime UTR, c.*52_*60del] and APOC3 rs138326449-11:116830638:G>A [donor loss, c.55+1G>A] variants.

A: Volcano plot displaying the results of ANGPTL3 cis-pQTL phenome-wide MR. B: APOC3 cis-pQTL phenome-wide MR volcano plot. The y-axis solid straight lines indicate the phenome-wide significance threshold. ‘OR’ indicates the odds ratio with 95% confidence intervals with Bonferroni correction for the 694 FinnGen outcomes.

Figure S5. Results of functional variant triglycerides-mediated CAD MR analyses of ANGPTL3 and ANGPTL4.

Forest plot and table displaying the results of the CAD MR analyses limiting instrument selection to functional variants in ANGPTL3 and ANGPTL4.

Supplemental Tables

The Supplemental Tables 1-9 are located within the Supplemental Tables .xlsx file.

Supplemental Table 1. Description of GWAS data sets

List of the GWAS data sets used. 'database.ID' denotes the EBI GWAS catalog identifiers if starting by "GCST", or the UK biobank showcase identifier if starting by a number.

Supplemental Table 2. MR results with 1000Genomes LD matrix

Results of the MR analyses that are presented in the paper. 'rsids.dbsnp.ver144' denote the rsids that were used in each MR model.

Supplemental Table 3. MR sensitivity analysis w. UKB 337K LD matrix vs 1000Genomes.

LD matrix sensitivity analysis using the 1000Genomes and UKB 337K LD matrices. 'het.beta' indicates whether the coefficients directionality differed between the two settings. 'heterogeneity.statistic' indicates the heterogeneity P-value, which is described in detail in the supplemental note.

Supplemental Table 4. MR sample overlap risk of bias analysis

Result of the risk of bias from sample overlap analysis reporting the F-statistics, bias ('Beta.bias.low.scenario', ' Beta.bias.medium.scenario', and ' Beta.bias.high.scenario') and type 1 error inflation (Type1error.lowbias.scenario, Type1error.mediumbias.scenario, Type1error.highbias.scenario) for each scenario and model.

Supplemental Table 5. ICD codes used for UKB lymphadenopathy-related phecodes

Phecode and ICD-codes as described in the Methods section.

Supplemental Table 6. ANGPTL4 p.40K pQTL MR PheWAS results

Detailed results of the MR analyses presented in **Figure 3D**.

Supplemental Table 7. ANGPTL4 p.Cys80fs pQTL MR PheWAS results

Detailed results of the MR analyses presented in **Figure 3D**.

Supplemental Table 8. *ANGPTL3 rs34483103-1:62604866:AGTTAATGTG>A* [3 prime UTR, c.*52_*60del]pQTL MR PheWAS results

Detailed results of the MR analyses presented in **Supplemental Figure 3A**.

Supplemental Table 9. ***APOC3 rs138326449-11:116830638:G>A*** **[donor loss, c.55+1G>A]pQTL**

MR PheWAS results

Detailed results of the MR analyses presented in **Supplemental Figure 3B**.

Study design

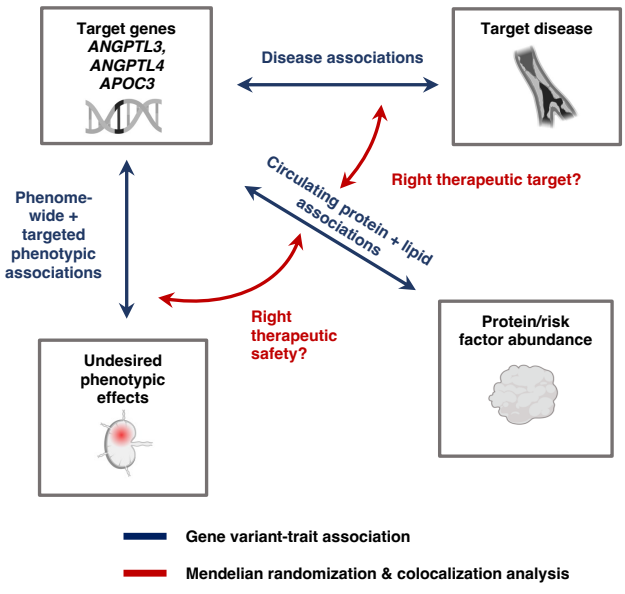

Key findings

		ANGPTL4	*ANGPTL3*	*APOC3*
Cardio-metabolic Disease	Chronic kidney disease	–	–	–
	Coronary artery disease	Improves	Improves	Improves
	Ischemic stroke	–	–	–
	Type 2 diabetes	Improves	–	–
	Non-alcoholic fatty liver disease	–	–	–
Safety	Routine labs	Weak	Weak	Weak
	Imaging	–	–	–
	Lymphadeno-pathies	–		
	Phenome-wide association study	Improves ASCVD and T2D outcomes		

Cardiometabolic diseases

A. Exposure: Target protein abundance

Outcome	Events/Total	Gene	No. SNPs	Odds ratio (95% CI)	P-value	Coloc.
Coronary artery disease	181,522 / 1,165,690	*ANGPTL3*	3	0.98 (0.91;1.06)	1.000	H1: 93%
		ANGPTL4	1	0.57 (0.47;0.70)	2e−19	H4: 100%
		APOC3	2	0.90 (0.82;0.99)	0.014	H3: 100%
		APOC3 c.55+1G>A	1	0.94 (0.84;1.05)	1.000	
Chronic kidney disease	41,395 / 480,698	*ANGPTL3*	3	0.97 (0.84;1.12)	1.000	H1: 94%
		ANGPTL4	1	0.99 (0.68;1.46)	1.000	H1: 94%
		APOC3	1	0.86 (0.62;1.19)	1.000	H1: 95%
		APOC3 c.55+1G>A	0			
Ischemic stroke	62,100 / 1,296,908	*ANGPTL3*	3	1.08 (0.97;1.21)	0.993	H1: 95%
		ANGPTL4	1	0.78 (0.56;1.09)	0.811	H1: 74%
		APOC3	1	0.97 (0.76;1.24)	1.000	H1: 94%
		APOC3 c.55+1G>A	0			
Non−alcoholic fatty liver disease	8,434 / 787,048	*ANGPTL3*	3	1.05 (0.81;1.37)	1.000	H1: 97%
		ANGPTL4	1	1.07 (0.60;1.91)	1.000	H1: 93%
		APOC3	1	0.91 (0.54;1.56)	1.000	H1: 94%
		APOC3 c.55+1G>A	0			
Type 2 diabetes	74,124 / 898,130	*ANGPTL3*	3	1.00 (0.91;1.11)	1.000	H1: 90%
		ANGPTL4	1	0.73 (0.57;0.94)	0.002	H4: 98%
		APOC3	2	1.00 (0.89;1.11)	1.000	H3: 57%
		APOC3 c.55+1G>A	1	1.08 (0.95;1.22)	1.000	
Type 2 diabetes adjusted for BMI	74,124 / 898,130	*ANGPTL3*	3	1.02 (0.90;1.14)	1.000	H1: 88%
		ANGPTL4	1	0.61 (0.46;0.80)	2e−07	H4: 100%
		APOC3	2	0.97 (0.85;1.10)	1.000	H3: 53%
		APOC3 c.55+1G>A	1	1.03 (0.89;1.20)	1.000	

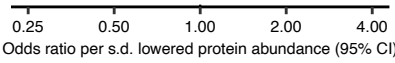

Odds ratio per s.d. lowered protein abundance (95% CI)

B. Exposure: Triglycerides

Coronary artery disease	181,522 / 1,165,690	*ANGPTL3*	3	0.96 (0.77;1.19)	1.00	H1: 96%
		ANGPTL4	3	0.43 (0.32;0.57)	2e−21	H4: 100%
		APOC3	7	0.80 (0.72;0.89)	6e−11	H4: 100%
		APOC3 c.55+1G>A	1	0.85 (0.64;1.13)	1.00	
		LPL	20	0.69 (0.61;0.77)	2e−24	H3: 100%
		Polygenic	117	0.76 (0.69;0.84)	1e−18	
Chronic kidney disease	41,395 / 480,698	*ANGPTL3*	3	0.85 (0.57;1.29)	1.00	H1: 94%
		ANGPTL4	3	0.97 (0.56;1.70)	1.00	H1: 94%
		APOC3	6	0.85 (0.68;1.06)	0.79	H1: 95%
		APOC3 c.55+1G>A	0			
		LPL	19	0.92 (0.74;1.14)	1.00	H1: 94%
		Polygenic	95	1.00 (0.87;1.14)	1.00	
Ischemic stroke	62,100 / 1,296,908	*ANGPTL3*	3	1.21 (0.89;1.65)	1.00	H1: 94%
		ANGPTL4	3	0.74 (0.46;1.19)	1.00	H1: 74%
		APOC3	6	0.99 (0.84;1.17)	1.00	H1: 95%
		APOC3 c.55+1G>A	0			
		LPL	14	0.97 (0.82;1.16)	1.00	H1: 96%
		Polygenic	89	0.98 (0.89;1.07)	1.00	
Non−alcoholic fatty liver disease	8,434 / 787,048	*ANGPTL3*	3	1.14 (0.55;2.37)	1.00	H1: 97%
		ANGPTL4	3	1.05 (0.45;2.46)	1.00	H1: 93%
		APOC3	5	0.96 (0.67;1.39)	1.00	H1: 95%
		APOC3 c.55+1G>A	0			
		LPL	14	0.66 (0.44;0.99)	0.03	H3: 52%
		Polygenic	83	0.92 (0.67;1.24)	1.00	
Type 2 diabetes	74,124 / 898,130	*ANGPTL3*	3	1.01 (0.76;1.33)	1.00	H1: 95%
		ANGPTL4	3	0.62 (0.43;0.89)	7e−04	H4: 98%
		APOC3	7	0.89 (0.77;1.01)	0.17	H3: 58%
		APOC3 c.55+1G>A	1	1.20 (0.88;1.65)	1.00	
		LPL	19	0.73 (0.63;0.86)	8e−10	H3: 51%
		Polygenic	104	0.87 (0.69;1.09)	1.00	
Type 2 diabetes adjusted for BMI	74,124 / 898,130	*ANGPTL3*	3	1.03 (0.74;1.44)	1.00	H1: 94%
		ANGPTL4	3	0.47 (0.31;0.71)	4e−08	H4: 100%
		APOC3	7	0.86 (0.73;1.01)	0.08	H3: 50%
		APOC3 c.55+1G>A	1	1.09 (0.74;1.60)	1.00	
		LPL	19	0.73 (0.61;0.86)	2e−08	H3: 76%
		Polygenic	103	0.80 (0.63;1.01)	0.08	

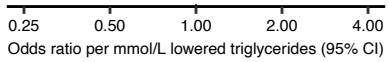

Odds ratio per mmol/L lowered triglycerides (95% CI)

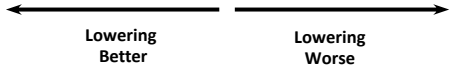

Cardiometabolic risk markers

Exposure: Target protein abundance

Outcome	Sample size	Gene	No. SNPs	Effect size (95% CI)	P-value	Coloc.
Total cholesterol	344,278	*ANGPTL3*	3	− 0.27 (−0.31;−0.23)	2e−107	H3: 100%
		ANGPTL4	1	0.09 (−0.01;0.18)	0.205	H3: 100%
		APOC3	2	− 0.08 (−0.12;−0.03)	5e−06	H3: 100%
		APOC3 c.55+1G>A	1	0.00 (−0.05;0.05)	1.000	
Triglycerides	343,992	*ANGPTL3*	3	− 0.34 (−0.38;−0.31)	6e−206	H3: 100%
		ANGPTL4	1	− 0.65 (−0.74;−0.56)	1e−125	H4: 100%
		APOC3	2	− 0.58 (−0.62;−0.53)	<2e−308	H3: 100%
		APOC3 c.55+1G>A	1	− 0.39 (−0.44;−0.35)	1e−155	
LDL cholesterol	343,621	*ANGPTL3*	3	− 0.15 (−0.19;−0.12)	2e−57	H3: 100%
		ANGPTL4	1	−0.02 (−0.10;0.06)	1.000	H1: 96%
		APOC3	2	− 0.10 (−0.14;−0.06)	7e−18	H3: 100%
		APOC3 c.55+1G>A	1	− 0.07 (−0.12;−0.03)	2e−07	
HDL cholesterol	315,133	*ANGPTL3*	3	− 0.02 (−0.03;−0.01)	4e−05	H3: 100%
		ANGPTL4	1	+ 0.24 (0.21;0.28)	8e−134	H4: 100%
		APOC3	2	+ 0.16 (0.14;0.17)	2e−238	H4: 100%
		APOC3 c.55+1G>A	1	+ 0.17 (0.15;0.18)	3e−206	
Apolipoprotein B	342,590	*ANGPTL3*	3	− 0.03 (−0.04;−0.03)	3e−36	H3: 100%
		ANGPTL4	1	−0.02 (−0.04;0.00)	0.041	H4: 58%
		APOC3	2	− 0.03 (−0.04;−0.02)	1e−22	H3: 100%
		APOC3 c.55+1G>A	1	− 0.02 (−0.03;−0.01)	7e−09	
Apolipoprotein A1	313,387	*ANGPTL3*	3	− 0.05 (−0.05;−0.04)	1e−51	H3: 100%
		ANGPTL4	1	+ 0.11 (0.09;0.14)	2e−55	H4: 100%
		APOC3	2	+ 0.07 (0.06;0.08)	8e−94	H3: 100%
		APOC3 c.55+1G>A	1	+ 0.10 (0.09;0.11)	3e−139	
Lipoprotein(a)	273,896	*ANGPTL3*	3	−0.09 (−2.14;1.96)	1.000	H1: 97%
		ANGPTL4	1	0.86 (−4.09;5.80)	1.000	H1: 96%
		APOC3	2	−0.99 (−3.33;1.36)	1.000	H1: 95%
		APOC3 c.55+1G>A	1	−0.19 (−2.86;2.48)	1.000	
Hemoglobin A1c	344,182	*ANGPTL3*	3	−0.02 (−0.25;0.22)	1.000	H1: 96%
		ANGPTL4	1	−0.47 (−1.04;0.10)	0.311	H1: 80%
		APOC3	2	0.06 (−0.21;0.33)	1.000	H1: 92%
		APOC3 c.55+1G>A	1	0.14 (−0.16;0.45)	1.000	
Systolic blood pressure	757,601	*ANGPTL3*	3	0.16 (−0.31;0.63)	1.000	H1: 99%
		ANGPTL4	1	−1.17 (−2.35;0.01)	0.056	H1: 55%
		APOC3	1	− 1.43 (−2.50;−0.36)	6e−04	H3: 100%
		APOC3 c.55+1G>A	0			
Diastolic blood pressure	757,601	*ANGPTL3*	3	−0.03 (−0.30;0.23)	1.000	H1: 100%
		ANGPTL4	1	−0.50 (−1.18;0.18)	0.755	H3: 100%
		APOC3	1	− 0.81 (−1.43;−0.20)	7e−04	H3: 100%
		APOC3 c.55+1G>A	0			
Waist to hip−ratio adj. for BMI	694,649	*ANGPTL3*	3	0.00 (−0.03;0.03)	1.000	H1: 96%
		ANGPTL4	1	− 0.12 (−0.19;−0.04)	2e−05	H4: 93%
		APOC3	2	0.02 (−0.02;0.05)	1.000	H3: 99%
		APOC3 c.55+1G>A	1	0.03 (−0.01;0.07)	1.000	
Waist to hip−ratio	697,734	*ANGPTL3*	3	−0.01 (−0.04;0.01)	1.000	H1: 95%
		ANGPTL4	1	− 0.09 (−0.16;−0.01)	0.005	H4: 86%
		APOC3	2	0.01 (−0.02;0.05)	1.000	H3: 98%
		APOC3 c.55+1G>A	1	0.02 (−0.02;0.06)	1.000	
Body fat percentage	454,633	*ANGPTL3*	3	−0.01 (−0.03;0.01)	1.000	H1: 99%
		ANGPTL4	1	+ 0.07 (0.01;0.12)	0.009	H4: 78%
		APOC3	1	0.03 (−0.03;0.08)	1.000	H3: 100%
		APOC3 c.55+1G>A	0			
Body mass index	806,834	*ANGPTL3*	3	−0.02 (−0.05;0.00)	0.143	H1: 93%
		ANGPTL4	1	0.01 (−0.06;0.09)	1.000	H1: 95%
		APOC3	2	0.00 (−0.04;0.03)	1.000	H3: 100%
		APOC3 c.55+1G>A	1	−0.01 (−0.05;0.03)	1.000	

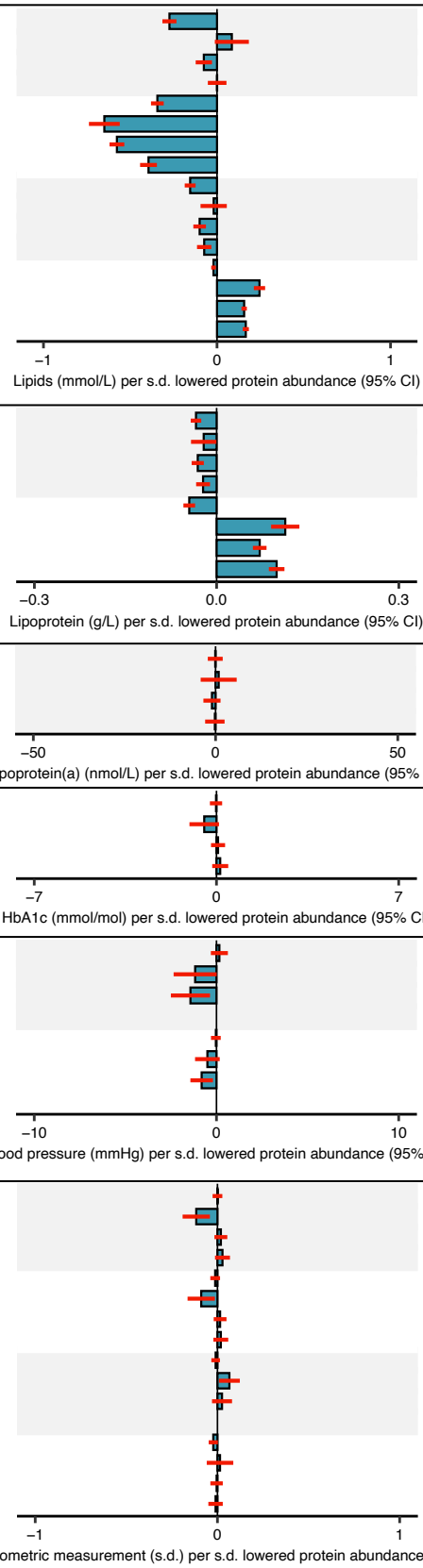

Safety

A. Imaging

Outcome	Sample size	ANGPTL3 Effect size (95% CI)	ANGPTL3 P-value	ANGPTL4 Effect size (95% CI)	ANGPTL4 P-value	APOC3 Effect size (95% CI)	APOC3 P-value
Abdominal scWAT vol.	32,860	0.01 (−0.10;0.11)	1	0.16 (−0.09;0.41)	1.0	−0.07 (−0.32;0.18)	1
Kidney volume	32,860	0.04 (−0.05;0.13)	1	0.13 (−0.09;0.35)	1.0	−0.13 (−0.35;0.09)	1
Liver fat percentage	32,858	0.05 (−0.07;0.16)	1	0.03 (−0.24;0.30)	1.0	0.01 (−0.26;0.28)	1
Liver iron	32,858	0.04 (−0.07;0.15)	1	−0.15 (−0.42;0.12)	1.0	−0.07 (−0.33;0.20)	1
Liver volume	32,860	0.06 (−0.05;0.16)	1	0.03 (−0.22;0.27)	1.0	0.01 (−0.23;0.25)	1
Lung volume	32,860	0.03 (−0.07;0.12)	1	0.06 (−0.18;0.30)	1.0	0.11 (−0.13;0.34)	1
Pancreas fat	25,617	0.02 (−0.10;0.15)	1	0.16 (−0.14;0.46)	1.0	−0.03 (−0.32;0.27)	1
Pancreas iron	25,617	0.03 (−0.10;0.16)	1	0.03 (−0.28;0.33)	1.0	0.07 (−0.23;0.37)	1
Pancreas volume	31,758	−0.03 (−0.14;0.08)	1	0.11 (−0.16;0.37)	1.0	−0.12 (−0.38;0.14)	1
Spleen volume	32,860	−0.04 (−0.15;0.06)	1	0.01 (−0.24;0.25)	1.0	0.05 (−0.19;0.29)	1
Visceral WAT volume	32,860	0.04 (−0.06;0.13)	1	0.19 (−0.04;0.43)	0.3	−0.06 (−0.29;0.17)	1

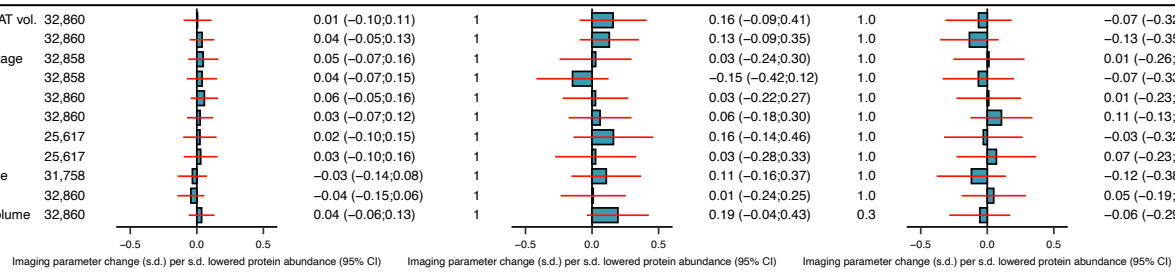

B. Blood chemistry

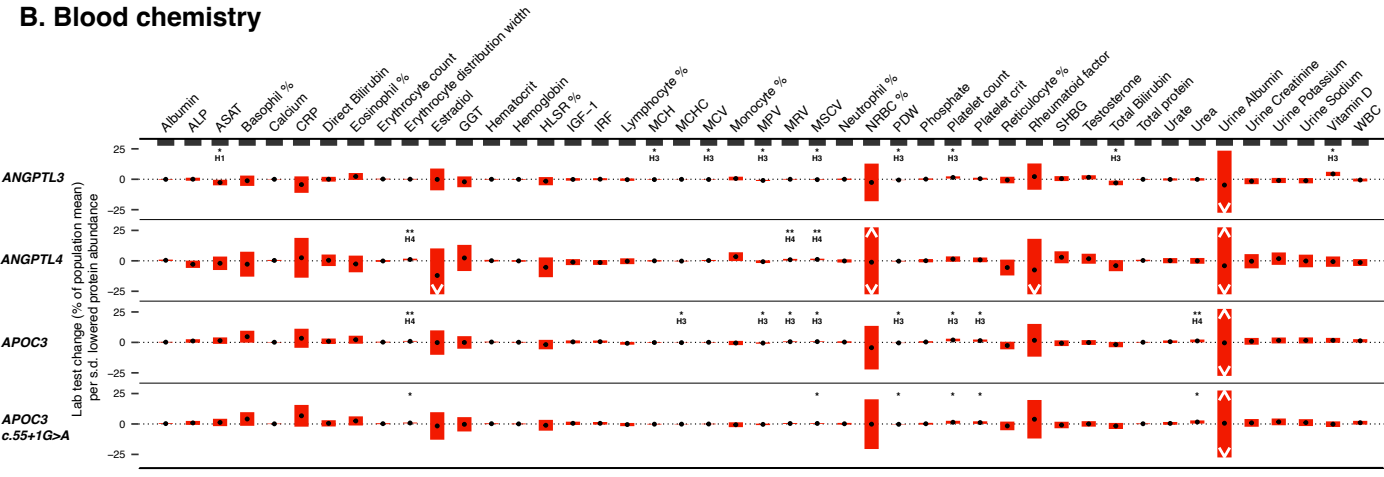

C. Lymphadenopathy

Variant	Outcome	Events/Total	Odds ratio (95% CI)	P-value
ANGPTL4 p.E40K	Acute lymphadenitis	6,597 / 700,506	1.03 (0.74;1.44)	0.9
	Acute peritonitis	3,362 / 689,698	0.77 (0.46;1.29)	0.3
	Ascites (non malignant)	3,384 / 367,211	1.13 (0.66;1.93)	0.7
	Intestinal malabsorption	1,693 / 600,069	0.99 (0.50;1.97)	1.0
	Noninfectious disorders of the lymphatic system	2,809 / 680,456	1.18 (0.69;2.00)	0.6
ANGPTL4 p.Cys80fs	Acute lymphadenitis	1,615 / 325,625	1.22 (0.96;1.55)	0.1
	Acute peritonitis	1,643 / 341,350	1.11 (0.87;1.41)	0.4
	Intestinal malabsorption	1,073 / 329,277	1.03 (0.77;1.38)	0.8
	Noninfectious disorders of the lymphatic system	798 / 295,812	1.01 (0.71;1.43)	1.0

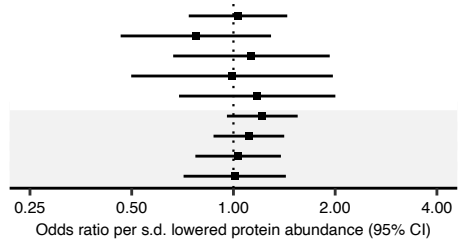

D. PheWAS

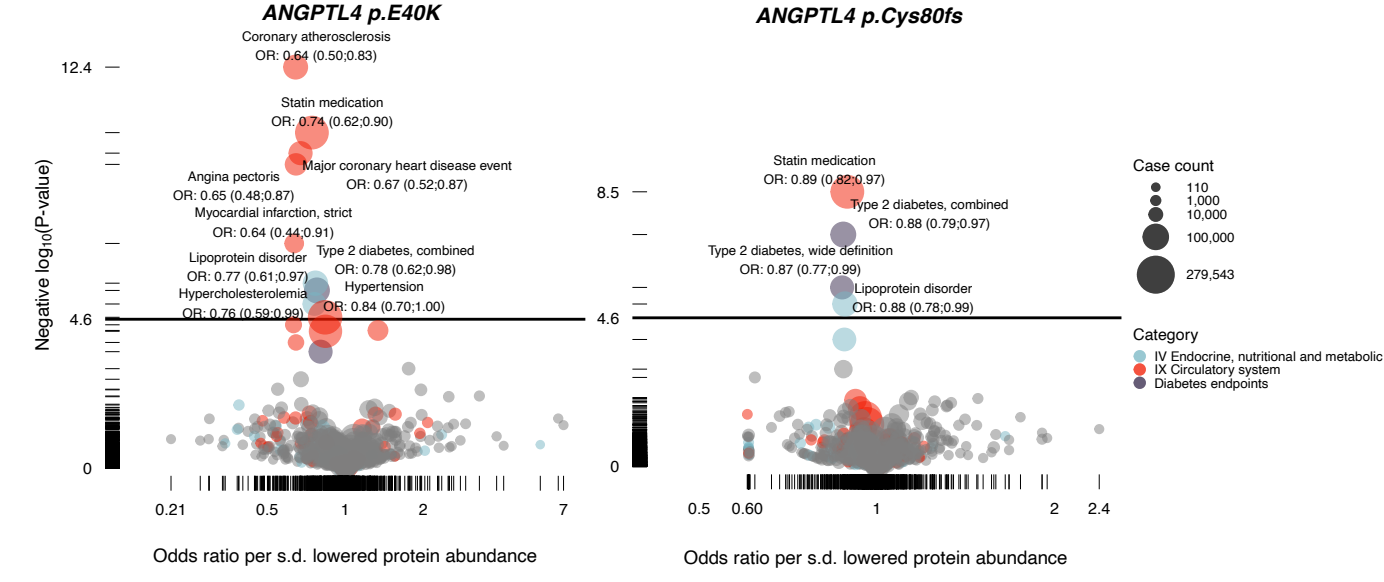

Metabolic Concordance of Protein-Truncating Variants vs. Common Variants

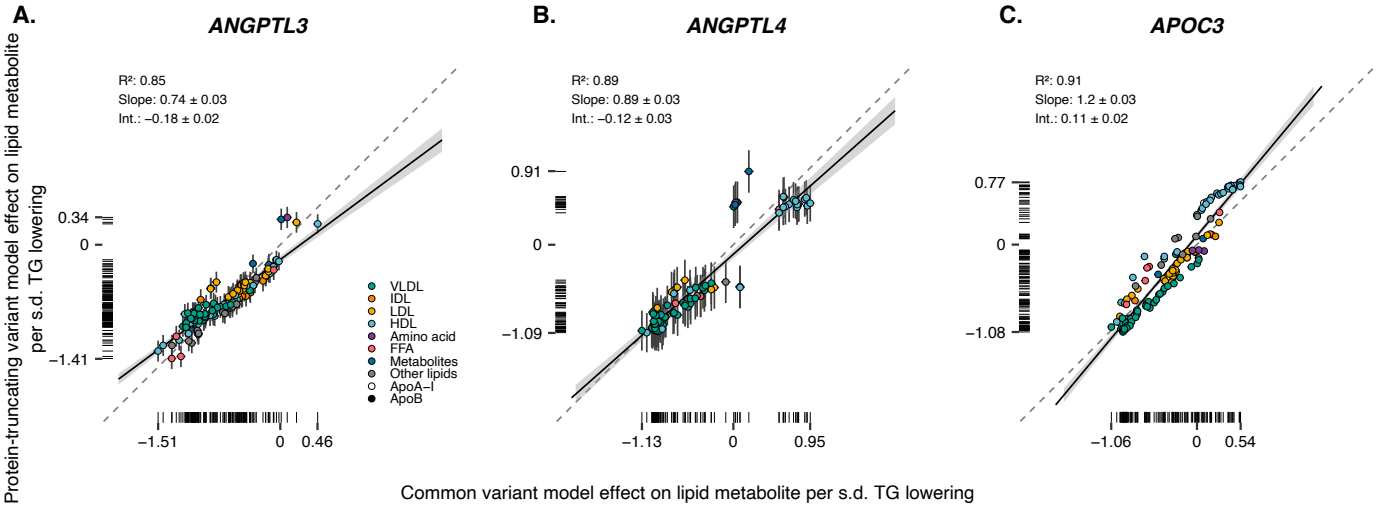

D. Coronary artery disease MR of *LPL* and *LIPG* restricted to functional variants

LIPG

Variant	Consequence	Events / Total	Freq.	Method	Odds ratio [95% CI] (P-value)	PL (s.d.)	TG (s.d.)	LDL-C (s.d.)	HDL-C (s.d.)
					Variant effect on plasma lipids [95% CI]				
18:49562285:T>G	5 prime UTR premature start codon gain	180,249 / 1,162,820	0.3206 (0.98)	Wald ratio	1.67 [1.09;2.57] (P=0.020)	0.02 [0.02;0.03]	–	–	0.03 [0.03;0.04]
18:49575468:G>A	Missense [p.Arg224His] SIFT: deleterious	53,953 / 544,132	0.0005 (0.7)	Wald ratio	0.77 [0.25;2.39] (P=0.647)	0.37 [0.15;0.59]	–	–	0.38 [0.27;0.48]
18:49583585:A>G	Missense [p.Asn396Ser] PolyPhen: probably damaging	170,178 / 1,133,320	0.0123 (0.98)	Wald ratio	1.34 [1.15;1.56] (P=2e−04)	0.30 [0.26;0.34]	0.04 [0.02;0.06]	0.07 [0.05;0.09]	0.29 [0.27;0.31]
18:49586795:C>T	Missense [p.Arg476Trp] SIFT: deleterious	123,638 / 933,548	0.0023 (0.96)	Wald ratio	1.50 [1.13;1.98] (P=0.004)	0.47 [0.38;0.56]	0.07 [0.02;0.11]	0.11 [0.06;0.15]	0.40 [0.35;0.44]
	Combined (Heterogeneity: Q=2.28; P=0.52)				**1.38 [1.22;1.57] (P=5e−07)**				

0.25 0.50 1.00 2.00 4.00

Coronary artery disease odds ratio per s.d. lowered total lipoprotein phospholipids (95% CI)

LPL

Variant	Consequence	Events / Total	Freq.	Method	Odds ratio [95% CI] (P-value)	TG (s.d.)		HDL-C (s.d.)
8:19954222:G>A	Missense [p.Gly215Glu] PolyPhen: probably damaging	65,057 / 568,082	0.0006 (1)	Wald ratio	0.48 [0.30;0.77] (P=0.002)	0.60 [0.41; 0.80]	–	–0.80 [–0.90;–0.71]
8:19962213:C>G	Stop gained [p.Ser474Ter] paradox. gain–of–function	177,063 / 1,157,050	0.0974 (1)	Wald ratio	0.75 [0.69;0.82] (P=2e−11)	–0.19 [–0.21;–0.18]	–	0.17 [0.17; 0.18]
	Combined (Heterogeneity: Q=3.37; P=0.066)				**0.74 [0.64;0.86] (P=1e−04)**			

0.25 0.50 1.00 2.00 4.00

Coronary artery disease odds ratio per s.d. lowered triglycerides (95% CI)

E. Coronary artery disease *cis*-pQTL MR of *ANGPTL3* and *ANGPTL4* restricted to functional variants

ANGPTL3

Variant	Consequence	Events / Total	Freq. (info)	Method	Odds ratio [95% CI] (P-value)	Protein (s.d.)	TG (s.d.)	LDL-C (s.d.)	HDL-C (s.d.)
					Variant effect on protein abundance / plasma lipids [95% CI]				
1:62597794:C>G	Missense [p.Asn76Lys] PolyPhen: possibly damaging	98,456 / 922,234	0.0114 (0.85)	Wald ratio	0.90 [0.81;1.00] (P=0.05)	–0.84 [–0.96;–0.71]	–	–	0.10 [0.05; 0.14]
1:62598067:T>C	Splice region [c.495+6T>C] SpliceAI: donor loss	80,569 / 895,497	0.0019 (0.93)	Wald ratio	1.00 [0.88;1.13] (P=0.99)	–1.50 [–1.69;–1.31]	–0.49 [–0.56;–0.42]	–0.25 [–0.32;–0.18]	–0.11 [–0.18;–0.04]
1:62601804:G>T	Missense [p.Gly253Cys] SIFT: deleterious	63,005 / 562,146	0.0007 (0.87)	Wald ratio	1.06 [0.82;1.37] (P=0.66)	–1.56 [–1.98;–1.14]	–0.47 [–0.63;–0.32]	–0.22 [–0.38;–0.06]	–
1:62604032:G>A	Missense [p.Arg332Gln] SIFT: deleterious	38,405 / 492,981	0.0022 (0.61)	Wald ratio	0.99 [0.90;1.09] (P=0.83)	–2.53 [–3.16;–1.90]	–0.62 [–0.94;–0.30]	–	–
1:62604866:AGTTAATGTG>A	3 prime UTR [c.*52_*60del]	159,190 / 1,110,890	0.3402 (0.99)	Wald ratio	0.98 [0.94;1.02] (P=0.28)	–0.28 [–0.30;–0.27]	–0.08 [–0.08;–0.07]	–0.04 [–0.04;–0.03]	–0.01 [–0.02;–0.01]
	Combined (Heterogeneity: Q=2.85; P=0.58)				**0.98 [0.94;1.01] (P=0.13)**				

ANGPTL4

19:8364439:G>A	Missense [p.Glu40Lys] SIFT: deleterious	164,838 / 1,122,180	0.0224 (0.86)	Wald ratio	0.60 [0.54;0.67] (P=4e−21)	–0.35 [–0.39;–0.30]	–0.23 [–0.24;–0.21]	–	0.20 [0.19;0.22]
19:8371489:C>T	Missense [p.Arg336Cys] SIFT: deleterious	132,683 / 975,311	0.0028 (0.98)	Wald ratio	0.82 [0.71;0.95] (P=0.009)	–0.77 [–0.89;–0.65]	–0.08 [–0.12;–0.04]	–	0.09 [0.05;0.13]
	Combined (Heterogeneity: Q=11.54; P=0.00068)				**0.67 [0.50;0.89] (P=0.007)**				

0.5 1.0 2.0

Coronary artery disease odds ratio per s.d. lowered protein abundance (95% CI)

Lowering Better ← → Lowering Worse

Meta-analysis of Coronary Artery Disease vs. Loss-of-Function Variants in DNA Sequencing Studies

ANGPTL3

Study	Ancestry	Coronary artery disease: Carriers	Coronary artery disease: Non-Carriers	Control: Carriers	Control: Non-Carriers	Per mmol/L TG: Odds ratio [95% CI] (P-value)	Per allele: Odds ratio [95% CI] (P-value)	TG reduction (~mmol/L)
BioImage study	Eur.	0	54	2	349	1.70 [0.00; 1196] (P=1)	1.28 [0.06; 27.2] (P=1)	–
Registre Gironi del COR	Eur.	2	380	1	401	4.96 [0.03; 867] (P=1)	2.11 [0.19; 23.4] (P=1)	–
South German Myocardial Infarction study	Eur.	0	400	1	398	0.09 [0.00; 123] (P=0.52)	0.33 [0.01; 9.43] (P=0.52)	–
Jackson Heart Study	Eur.	1	133	11	2031	2.03 [0.02; 164] (P=1)	1.39 [0.18; 10.8] (P=1)	–
Exome Sequencing Project Early–Onset Myocardial Infarction	Afr.	1	172	4	674	0.96 [0.01; 106] (P=0.99)	0.98 [0.11; 8.78] (P=0.99)	–
North German Myocardial Infarction study	Eur.	4	853	2	869	4.62 [0.12; 178] (P=1)	2.04 [0.37; 11.2] (P=1)	–
Ottawa Heart Study	Eur.	0	956	2	964	0.03 [0.00; 20.7] (P=0.3)	0.20 [0.01; 4.10] (P=0.3)	–
Atherosclerosis Risk in Communities	Afr.	1	391	8	2590	0.67 [0.01; 60.4] (P=0.86)	0.83 [0.10; 6.76] (P=0.86)	–
Precocious Coronary Artery Disease study	Eur.	4	909	3	901	1.81 [0.07; 46.1] (P=1)	1.32 [0.29; 5.96] (P=1)	–
Atherosclerosis Risk in Communities	Eur.	0	773	18	6464	0.04 [0.00; 24.7] (P=0.33)	0.23 [0.01; 4.45] (P=0.33)	–
Italian Atherosclerosis Thrombosis and Vascular Biology	Eur.	6	1763	5	1694	1.35 [0.10; 17.4] (P=1)	1.15 [0.35; 3.78] (P=1)	–
Exome Sequencing Project Early–Onset Myocardial Infarction	Eur.	3	567	9	1389	0.65 [0.04; 10.9] (P=0.77)	0.82 [0.22; 3.04] (P=0.77)	–
Leicester Myocardial Infarction study	Eur.	2	1218	6	1090	0.08 [0.00; 2.35] (P=0.14)	0.30 [0.06; 1.49] (P=0.14)	–
Pakistan Risk of Myocardial Infarction Study	Sas.	10	4765	20	5651	0.32 [0.06; 1.63] (P=0.17)	0.59 [0.28; 1.26] (P=0.17)	–
Geisinger Health System (DiscovEHR)	Eur.	43	13059	183	40247	0.27 [0.11; 0.67] (P=0.0046)	0.59 [0.41; 0.85] (P=0.0046)	−0.41 [CI: −0.49; −0.32]
Copenhagen General Population Studies	Eur.	10	11162	131	96585	0.37 [0.09; 1.57] (P=0.18)	0.63 [0.32; 1.24] (P=0.18)	–
University of Pennsylvania Medicine Biobank	Eur.	8	3983	20	3538	0.18 [0.02; 1.31] (P=0.09)	0.45 [0.18; 1.13] (P=0.09)	–
Duke Catheterization Genetics cohort	Eur.	12	4507	3	1466	1.84 [0.11; 30.1] (P=1)	1.33 [0.36; 4.88] (P=1)	–
Taiwan Metabochip consortium	Eas.	3	3632	4	5419	0.35 [0.01; 9.83] (P=0.53)	0.61 [0.13; 2.90] (P=0.53)	–
United Kingdom Biobank	Eur.	151	43121	496	106129	0.54 [0.37; 0.79] (P=0.0016)	0.74 [0.62; 0.89] (P=0.0016)	−0.48 [CI: −0.51; −0.44]
Pooled estimate (Heterogeneity: Q=6.11; P=1)		**261**	**92798**	**929**	**278849**	**0.45 [0.33; 0.61] (P=5.3e−07)**	**0.71 [0.62; 0.82] (P=4.6e−06)**	**−0.47 [CI: −0.50; −0.43]**

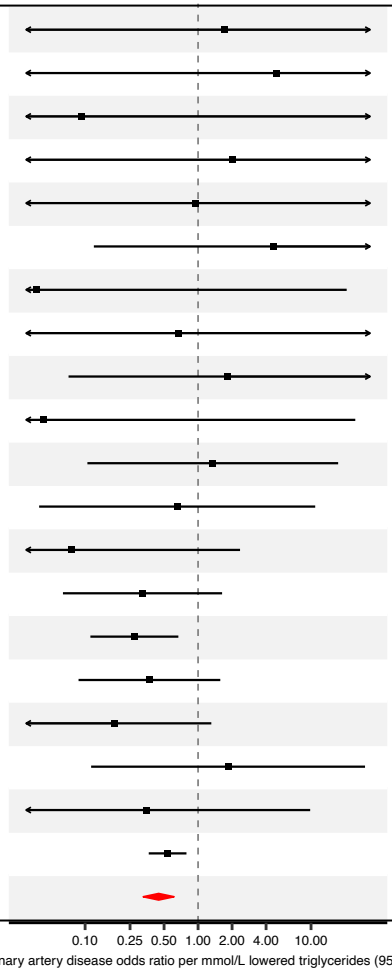

ANGPTL4 (Excluding *ANGPTL4* p.E40K)

Study	Ancestry	Coronary artery disease: Carriers	Coronary artery disease: Non-Carriers	Control: Carriers	Control: Non-Carriers	Per mmol/L TG: Odds ratio [95% CI] (P-value)	Per allele: Odds ratio [95% CI] (P-value)	TG reduction (~mmol/L)
Geisinger Health System (DiscovEHR)	Eur.	13	10539	58	29165	0.05 [0.00; 0.95] (P=0.046)	0.56 [0.32; 0.99] (P=0.046)	−0.19 [CI: −0.35; −0.03]
United Kingdom Biobank	Eur.	115	43157	347	106278	0.42 [0.17; 1.03] (P=0.059)	0.82 [0.66; 1.01] (P=0.059)	−0.24 [CI: −0.29; −0.18]
Pooled estimate (Heterogeneity: Q=1.87; P=0.17)		**128**	**53696**	**405**	**135443**	**0.35 [0.15; 0.83] (P=0.017)**	**0.78 [0.64; 0.95] (P=0.014)**	**−0.23 [CI: −0.28; −0.18]**

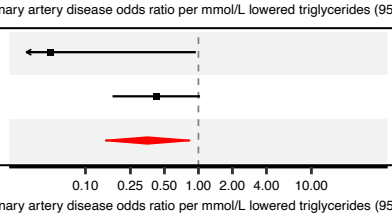

APOC3

Study	Ancestry	Coronary artery disease: Carriers	Coronary artery disease: Non-Carriers	Control: Carriers	Control: Non-Carriers	Per mmol/L TG: Odds ratio [95% CI] (P-value)	Per allele: Odds ratio [95% CI] (P-value)	TG reduction (~mmol/L)
Copenhagen City Heart Study	Eur.	9	2808	32	7484	0.55 [0.25; 1.19] (P=0.13)	0.60 [0.31; 1.16] (P=0.13)	–
United Kingdom Biobank	Eur.	198	43074	575	106050	0.82 [0.68; 1.00] (P=0.046)	0.85 [0.72; 1.00] (P=0.046)	−0.85 [CI: −0.88; −0.82]
Pooled estimate (Heterogeneity: Q=0.99; P=0.32)		**207**	**45882**	**607**	**113534**	**0.80 [0.67; 0.97] (P=0.021)**	**0.83 [0.71; 0.97] (P=0.021)**	**−0.85 [CI: −0.88; −0.82]**